Immunity

Targeted removal of macrophage-secreted interleukin-1 receptor antagonist protects against lethal *Candida albicans* sepsis

Graphical abstract

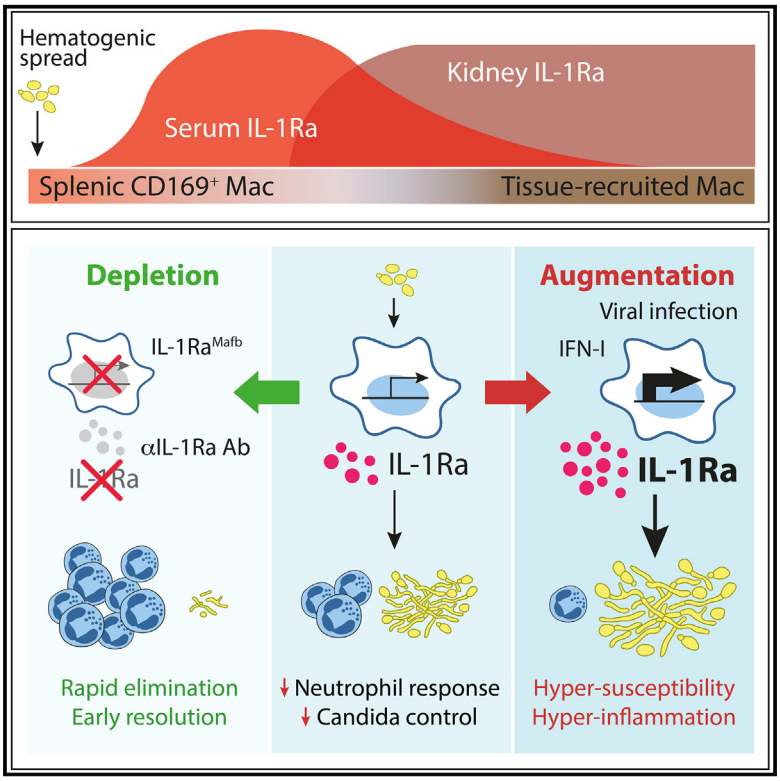

Highlights

- IL-1Ra is an innate immune checkpoint that facilitates invasive *Candida* infection
- Splenic CD169^{+} marginal zone macrophages secrete IL-1Ra into the bloodstream
- Therapeutic neutralization of IL-1Ra protects against fatal *C. albicans* sepsis
- Type I interferon amplifies macrophage IL-1Ra and exacerbates fungal dissemination

Authors

Hang Thi Thuy Gander-Bui, Joëlle Schläfli, Johanna Baumgartner, ..., Hans Christian Probst, Cem Gabay, Stefan Freigang

Correspondence

stefan.freigang@unibe.ch

In brief

Invasive candidiasis has high mortality rates with limited therapeutic options. Gander-Bui et al. show how macrophage-secreted IL-1 receptor antagonist (IL-1Ra) restricts recruitment of fungicidal neutrophils and drives candidiasis pathology. Therapeutic IL-1Ra neutralization protects against lethal Candida sepsis; however, interferon-driven amplification of IL-1Ra during viral infection exacerbates fungal dissemination and disease.

Gander-Bui et al., 2023, Immunity *56*, 1–18
August 8, 2023
https://doi.org/10.1016/j.immuni.2023.06.023

CellPress

Immunity

CellPress
OPEN ACCESS

Article

Targeted removal of macrophage-secreted interleukin-1 receptor antagonist protects against lethal *Candida albicans* sepsis

Hang Thi Thuy Gander-Bui,[1,2] Joëlle Schläfli,[1] Johanna Baumgartner,[1,2] Sabrina Walthert,[1] Vera Genitsch,[3] Geert van Geest,[4] José A. Galván,[3] Carmen Cardozo,[3] Cristina Graham Martinez,[3] Mona Grans,[5] Sabine Muth,[5] Rémy Bruggmann,[4] Hans Christian Probst,[5] Cem Gabay,[6] and Stefan Freigang[1,7,*]

[1]Division of Experimental Pathology, Institute of Tissue Medicine and Pathology, University of Bern, 3008 Bern, Switzerland
[2]Graduate School for Cellular and Biomedical Sciences, University of Bern, 3012 Bern, Switzerland
[3]Institute of Tissue Medicine and Pathology, University of Bern, 3008 Bern, Switzerland
[4]Interfaculty Bioinformatics Unit and Swiss Institute of Bioinformatics, University of Bern, 3012 Bern, Switzerland
[5]Institute for Immunology, University Medical Center Mainz, 55131 Mainz, Germany
[6]Division of Rheumatology, Department of Medicine, University Hospital of Geneva, 1211 Geneva, Switzerland
[7]Lead contact
*Correspondence: stefan.freigang@unibe.ch
https://doi.org/10.1016/j.immuni.2023.06.023

SUMMARY

Invasive fungal infections are associated with high mortality rates, and the lack of efficient treatment options emphasizes an urgency to identify underlying disease mechanisms. We report that disseminated *Candida albicans* infection is facilitated by interleukin-1 receptor antagonist (IL-1Ra) secreted from macrophages in two temporally and spatially distinct waves. Splenic CD169^{+} macrophages release IL-1Ra into the bloodstream, impeding early neutrophil recruitment. IL-1Ra secreted by monocyte-derived tissue macrophages further impairs pathogen containment. Therapeutic IL-1Ra neutralization restored the functional competence of neutrophils, corrected maladapted hyper-inflammation, and eradicated the otherwise lethal infection. Conversely, augmentation of macrophage-secreted IL-1Ra by type I interferon severely aggravated disease mortality. Our study uncovers how a fundamental immunoregulatory mechanism mediates the high disease susceptibility to invasive candidiasis. Furthermore, interferon-stimulated IL-1Ra secretion may exacerbate fungal dissemination in human patients with secondary candidemia. Macrophage-secreted IL-1Ra should be considered as an additional biomarker and potential therapeutic target in severe systemic candidiasis.

INTRODUCTION

Sepsis is a severe, life-threatening condition triggered by microbial dissemination via the bloodstream and a maladapted systemic inflammatory response.[1] Although fungal sepsis is less frequent, invasive fungal infections have particularly high mortality rates.[2,3] *Candida albicans* represents the most common cause of fungal bloodstream infection; and despite adequate antifungal treatment, the overall mortality is 30%–40%, exceeding 60% in critically ill patients.[4,5] *C. albicans* is normally contained by epithelial barrier immunity and occurs as commensal in half of the population.[6–8] Inborn errors of immunity highlight the importance of interleukin (IL)-17-mediated pathways to avert mucocutaneous colonization, whereas functional neutrophil responses are critical to prevent systemic infection.[9,10] Accordingly, individuals with immunosuppression due to hematologic malignancies, organ transplantation, AIDS, or prolonged intensive care hospitalization are highly susceptible to invasive candidiasis. However, preceding systemic viral infections,[11,12] or medical interventions that compromise physiological barrier function, such as indwelling devices, parenteral nutrition, and abdominal surgery, may predispose otherwise immuno-competent hosts to disseminated *Candida* infection.[4,5] Given the high mortality of invasive fungal infections, the emergence of drug resistant strains, and an increasing number of high-risk patients, there is great interest in defining underlying disease mechanisms to develop novel therapeutic strategies.[2,4]

Inflammation is the physiological innate response to tissue damage aiming to eliminate the injuring agent and restore internal homeostasis.[13] Both, the dynamics and the composition of its powerful effector functions must be precisely adapted to the characteristics of the invading pathogen to provide appropriate defense mechanisms that ensure pathogen clearance while avoiding extensive tissue damage.[13] Therefore, interacting networks of pro- and anti-inflammatory cytokines orchestrate the differentiation and recruitment of functionally distinct immune cell populations. Moreover, there are negative feedback mechanisms, the so-called immune checkpoints, which signal

Please cite this article in press as: Gander-Bui et al., Targeted removal of macrophage-secreted interleukin-1 receptor antagonist protects against lethal *Candida albicans* sepsis, Immunity (2023), https://doi.org/10.1016/j.immuni.2023.06.023

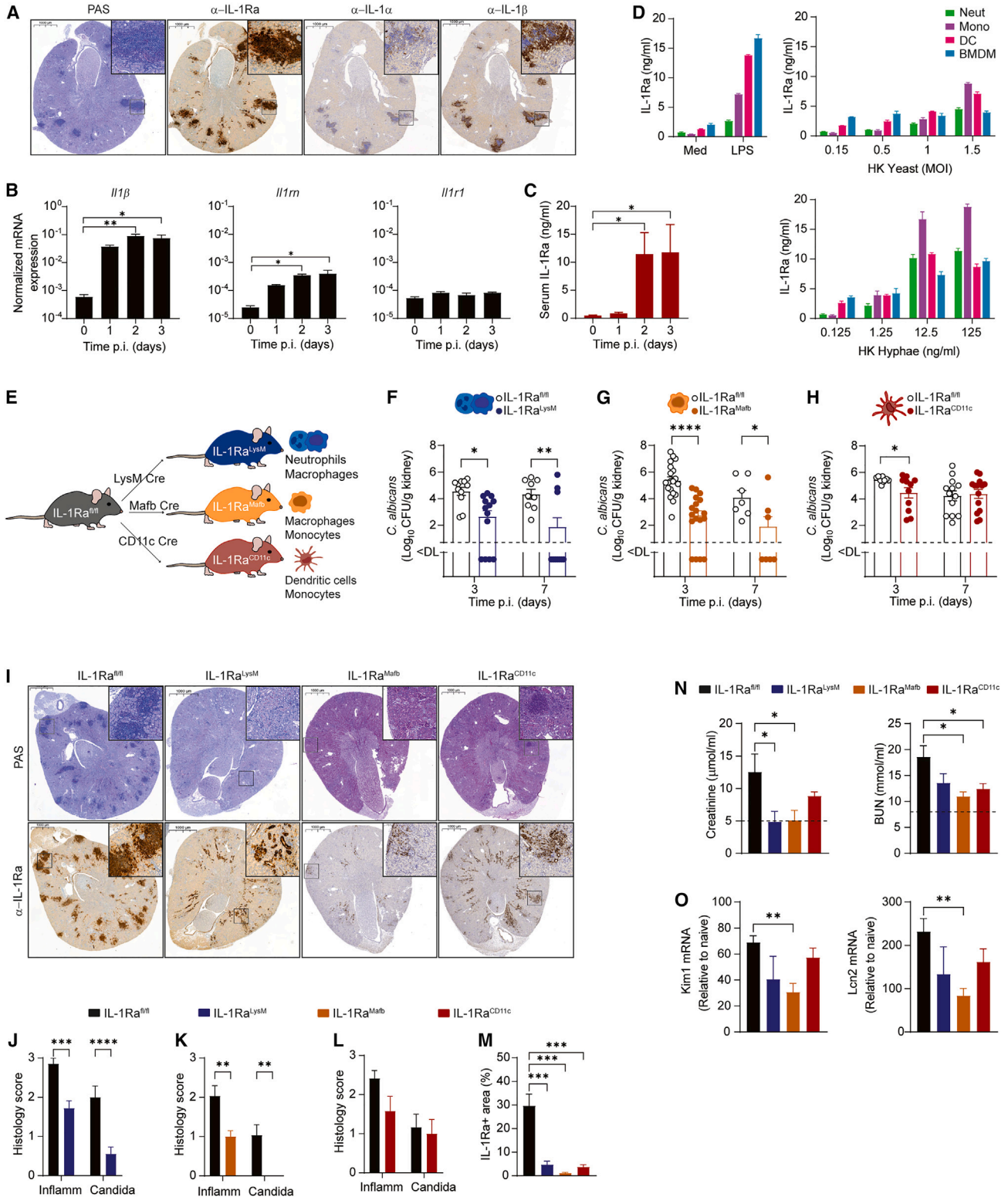

Figure 1. Ablation of macrophage-produced IL-1Ra protects against invasive fungal infection

(A) Representative periodic acid-Schiff (PAS), IL-1α, IL-1β, and IL-1Ra staining in the kidney at day 3 p.i. Scale bars, 1,000 μm.

(B) mRNA expression of IL-1β, IL-1Ra, and IL-1R in the kidney at indicated days p.i. (n = 4–8 mice/time point, two pooled experiments).

(C) Quantification of the serum IL-1Ra at indicated days p.i. (n = 12–20 mice/time point).

(D) IL-1Ra production by indicated myeloid cell subsets upon stimulation with LPS, heat-killed *C. albicans* yeast or hyphae *in vitro*.

(legend continued on next page)

Please cite this article in press as: Gander-Bui et al., Targeted removal of macrophage-secreted interleukin-1 receptor antagonist protects against lethal *Candida albicans* sepsis, Immunity (2023), https://doi.org/10.1016/j.immuni.2023.06.023

disproportionate immune activation and dampen the inflammatory process to prevent immunopathology. However, sepsis is characterized by a derailment of such pro- and anti-inflammatory pathway homeostasis with concurrent hyper-inflammation and immune paralysis, resulting in a dysfunctional systemic inflammatory response, multi-organ damage, and failure to contain pathogen replication.[14]

The prototypical pro-inflammatory cytokine IL-1 initiates and coordinates local and systemic inflammatory responses by activating the IL-1 receptor (IL-1R) on immune and non-immune cells.[15] Both IL-1 cytokines, IL-1α and IL-1β, are quintessential for antimicrobial immunity, including to *C. albicans*.[16–18] Still, excessive IL-1 production is associated with severe acute and chronic inflammatory conditions, such as autoinflammatory syndromes, rheumatoid arthritis, sepsis, or metabolic disorders.[19,20] Accordingly, IL-1α and IL-1β are subject to highly complex regulatory mechanisms acting at the transcriptional and posttranslational level, which restrict the generation of the mature cytokines or influence their ability to activate the IL-1R.[15,19] The inflammatory effects of bioactive IL-1α and IL-1β are controlled by the IL-1R antagonist (IL-1Ra), an endogenous inhibitor that competes for occupancy of the IL-1R but does not trigger downstream signaling.[19,21] One secreted and three intracellular isoforms of IL-1Ra have been described and are derived from the same *IL1RN* gene.[22] Adding to the complexity of IL-1 regulation, these individual isoforms are differentially expressed in various cell types. For example, intracellular IL-1Ra is constitutively expressed in epithelial cells, whereas secreted and intracellular isoforms may be induced in diverse leukocyte subsets in response to pro-inflammatory cytokines, microbial products, or tissue injury.[22] The potency of IL-1Ra-mediated regulation is evident in the severe inflammatory syndrome of deficiency of interleukin-1 receptor antagonist (DIRA) patients[23] and is exploited therapeutically for the management of IL-1-mediated diseases.[20] However, although the molecular pathways that govern the generation and secretion of mature IL-1 are well appreciated,[24–27] much less is known about the regulatory mechanisms operating at the level of receptor binding, such as IL-1Ra, particularly with respect to the cell-type-specific regulation of IL-1-driven inflammation.[28–30]

Here, we investigated the expression of IL-1Ra across different myeloid cell subsets in a murine model of invasive candidiasis and examined the impact of IL-1Ra produced by specific cell types on antifungal immunity. We showed that macrophage-secreted IL-1Ra acted as an innate immune checkpoint that prevented efficient pathogen clearance, and its targeted removal protected against lethal *C. albicans* sepsis. Moreover, we found that macrophage-secreted IL-1Ra was positively regulated by type I interferon (IFN), reflecting the association between secondary invasive candidiasis and preceding viral infections. Together, these results provide a mechanistic explanation for the high disease susceptibility to *Candida* bloodstream infection and suggest IL-1Ra-targeted therapies as a novel treatment approach.

RESULTS

IL-1Ra is rapidly expressed upon bloodstream infection with *C. albicans*

To establish the relevance of IL-1 signaling during invasive fungal infection, we examined IL-1 family cytokine expression in the kidney following intravenous infection with 2.5×10^5 colony-forming unit (CFU) *Candida albicans*. IL-1β and IL-1Ra protein were strongly expressed throughout infectious foci at day 3 post infection (p.i.), whereas few IL-1α positive cells were situated at the outer margin of lesions (Figure 1A). Transcripts for IL-1β were already present in the kidneys of naive animals; yet, IL-1R1 and IL-1Ra could only be detected at very low levels. However, fungal infection rapidly triggered increased gene expression of both IL-1β and IL-1Ra in the kidneys, whereas IL-1R1 mRNA expression stayed unchanged compared with naive mice (Figure 1B). Furthermore, substantial levels of IL-1Ra protein were present in the serum of infected mice and peaked at day 2 p.i. (Figure 1C). In contrast, mature IL-1β cytokine remained undetectable in the peripheral blood and was likely produced locally in infected tissues (Figure 1A and not shown). Expression of the IL-1Ra protein in the kidneys coincided with leukocyte recruitment and was limited to inflammatory infiltrates, suggesting immune cells as main IL-1Ra producers (Figures 1A, S1, and S2A). Indeed, primary neutrophils, monocytes, dendritic cells, and bone marrow (BM)-derived macrophages secreted IL-1Ra in response to both *Candida* morphotypes *in vitro*, with highest IL-1Ra levels elicited from monocytes exposed to *Candida* hyphae (Figure 1D). These data confirm the IL-1β/IL-1R1 axis as an important component of the early antifungal immune defense and implicate IL-1Ra produced by myeloid cells in its regulation.

Ablation of macrophage-produced IL-1Ra protects against invasive fungal infection

We therefore sought to dissect the impact of IL-1Ra produced by specific leukocyte subsets on the immune response to *C. albicans* using conditional deletion of IL-1Ra selectively in neutrophils, macrophages, or dendritic cells. We crossed IL-1Ra$^{fl/fl}$ mice[31] with respective Cre-driver strains to delete IL-1Ra in neutrophils and macrophages (LysM-Cre,[32] termed IL-1Ra^{LysM}), in macrophages (Mafb-Cre,[33] termed IL-1Ra^{Mafb}) and in CD11c-expressing cells (CD11c-Cre,[34] termed IL-1Ra^{CD11c})

(E) Generation of conditional IL-1Ra-deficient lines.
(F–H) *Candida* titers in the kidneys of IL-1Ra^{LysM}, IL-1Ra^{Mafb}, IL-1Ra^{CD11c}, and wild-type IL-1Ra$^{fl/fl}$ mice on days 3 and 7 p.i. ($n \geq 7$ mice/group, three pooled experiments).
(I) Representative PAS and IL-1Ra staining in the kidneys at day 3 p.i. Scale bars, 1,000 μm.
(J–M) Quantification of histopathological analysis (J–L) and IL-1Ra-positive areas (M) from (I).
(N) Plasma creatinine and BUN concentrations of indicated strains at day 2 p.i. Dashed lines indicate baselines (n = 7–13 mice/group, two pooled experiments).
(O) Quantification of renal Kim-1 and Lcn2 mRNA expression (n = 4–9 mice/group, two pooled experiments).
Error bars represent mean ± SEM. *p < 0.05; **p < 0.01; ***p < 0.001; ****p < 0.0001.
See also Figures S1–S3.

Please cite this article in press as: Gander-Bui et al., Targeted removal of macrophage-secreted interleukin-1 receptor antagonist protects against lethal *Candida albicans* sepsis, Immunity (2023), https://doi.org/10.1016/j.immuni.2023.06.023

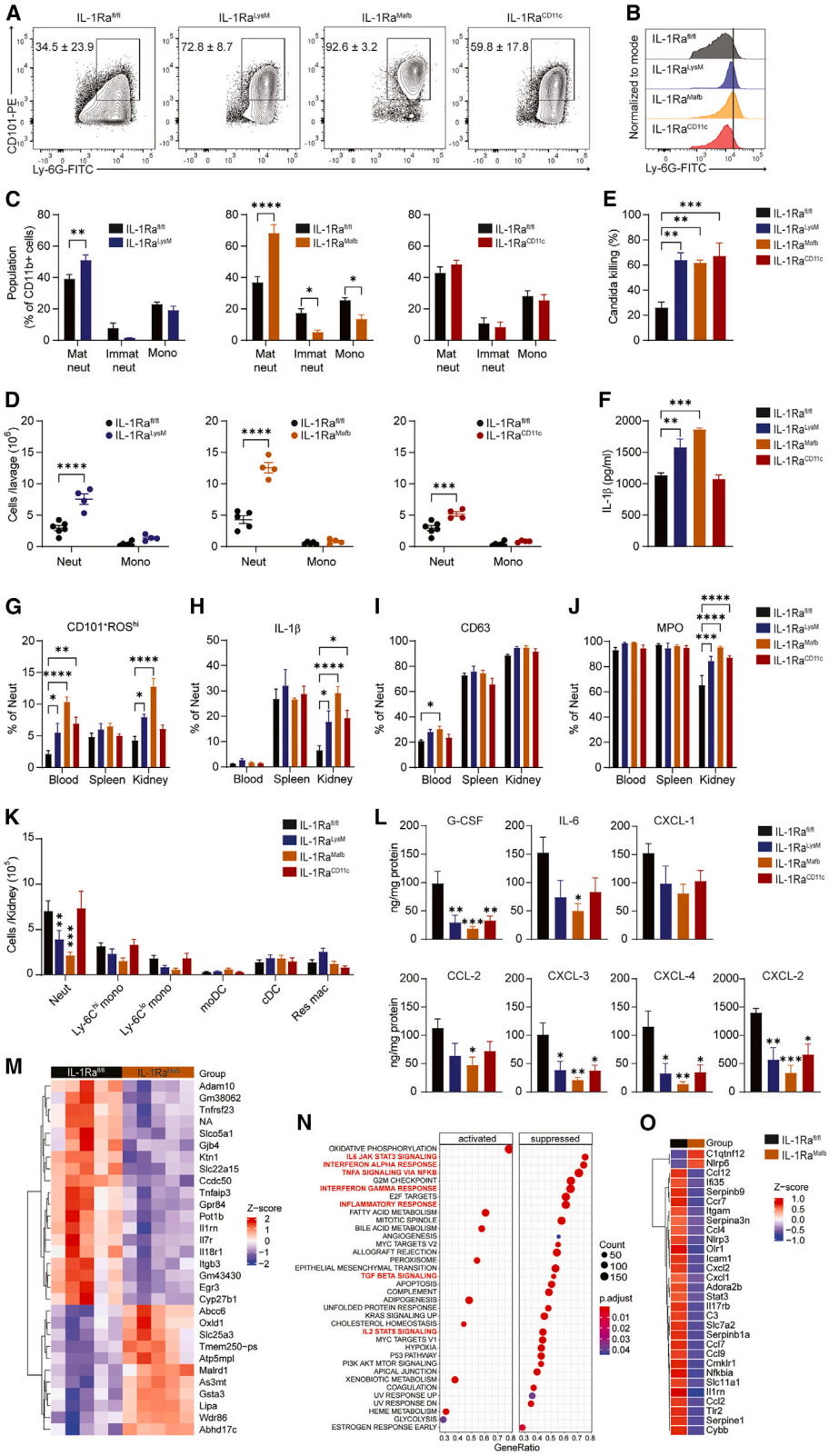

Figure 2. Macrophage-produced IL-1Ra prevents rapid neutrophil recruitment and inflammation resolution

(A–C) Analysis of blood leukocytes in indicated strains on day 2 p.i. for Ly-6G$^+$ CD101$^+$ expression (A) and Ly-6G fluorescence intensity (B) of neutrophils, and frequencies of mature neutrophils, immature neutrophils, and monocytes (C) (n = 6–8 mice/group, two pooled experiments).

(legend continued on next page)

Please cite this article in press as: Gander-Bui et al., Targeted removal of macrophage-secreted interleukin-1 receptor antagonist protects against lethal *Candida albicans* sepsis, Immunity (2023), https://doi.org/10.1016/j.immuni.2023.06.023

(Figures 1E, S3A, and S3B). Macrophage-specific ablation of IL-1Ra drastically improved the early immune control of *C. albicans* infection in IL-1Ra^{LysM} and IL-1Ra^{Mafb} mice compared with IL-1Ra$^{fl/fl}$ littermate controls (Figures 1F and 1G). Both strains reduced fungal titers in the kidneys already at day 3 p.i. and controlled *C. albicans* below the limit of detection in the majority of animals within 7 days. Although IL-1Ra^{LysM} mice lacked IL-1Ra in both macrophages and neutrophils, their phenotype was almost identical to that of IL-1Ra^{Mafb} mice lacking IL-1Ra selectively in macrophages.[33] In addition, macrophages and neutrophils of IL-1Ra^{LysM} mice exhibited residual IL-1Ra expression *in vivo* and *in vitro*, whereas IL-1Ra deletion was highly specific and efficient in macrophages of IL-1Ra^{Mafb} mice (Figures S2B, S3A, and S3B). This rendered major contributions of neutrophil-expressed IL-1Ra unlikely and identified macrophage-produced IL-1Ra as an important negative regulator of IL-1R signaling during systemic *Candida* infection. However, ablation of IL-1Ra in CD11c-expressing cells provided weaker and only transient protection. Although the kidneys of IL-1Ra^{CD11c} mice contained lower fungal loads than IL-1Ra$^{fl/fl}$ littermates at 3 days p.i., this difference had disappeared by day 7 (Figure 1H). Thus, IL-1Ra produced by CD11c-expressing cells influenced the initial antifungal defense but did not impact long-term control.

These observations were corroborated by the histopathological examination of infected kidneys (Figure 1I). Confirming their superior ability to contain fungal replication early on (Figures 1F and 1G), IL-1Ra^{LysM} and IL-1Ra^{Mafb} mice showed very restricted distribution of *C. albicans* and less inflammation in kidneys 3 days p.i. (Figures 1I–1K). Moreover, IL-1Ra^{LysM} and IL-1Ra^{Mafb} mice lost less weight compared with controls, which was indicative for their reduced general morbidity (Figure S3C). In comparison, IL-1Ra^{CD11c} mice exhibited an intermediate phenotype with reduced *Candida* dissemination and inflammation at day 3, but unaltered weight loss (Figures 1H, 1I, 1L, and S3C). Consistent with their improved immune control of *C. albicans*, we found markedly fewer infectious foci and reduced IL-1Ra-positive areas in kidney sections of all three IL-1Ra-deficient strains (Figures 1I–1M). The beneficial effect of IL-1Ra ablation in macrophages was most pronounced in IL-1Ra^{Mafb} mice, as illustrated by their reduced creatinine and blood urea nitrogen levels (Figure 1N) and lower expression of kidney injury markers Lcn2 and Kim-1 (Figure 1O). Altogether, our results establish that ablation of macrophage-produced IL-1Ra strongly improves the ability to control invasive *Candida* infection, resulting in rapid pathogen clearance, reduced disease severity, and a better preservation of organ function.

IL-1Ra controls the recruitment and fungicidal capacity of neutrophils

To investigate how removal of macrophage-produced IL-1Ra enabled the efficient containment of systemic candidiasis, we characterized antifungal immune responses in the respective IL-1Ra-deficient strains. Macrophage-specific deletion of IL-1Ra increased the early mobilization and maturation of neutrophils in IL-1Ra^{Mafb} and IL-1Ra^{LysM} mice, as indicated by greater proportions of mature CD101^{+} Ly-6G high neutrophils in the blood on day 2 p.i. (Figures 2A–2C). This effect was strongest in IL-1Ra^{Mafb} mice, which also showed reduced proportions of circulating immature neutrophils and inflammatory monocytes (Figure 2C).

The absence of macrophage-produced IL-1Ra also accelerated the recruitment of neutrophils to inflammatory sites. To exclude feedback mechanisms triggered by differential microbial control, we examined inflammatory responses to non-replicating fungal cell wall components. The peritoneal lavages of zymosan-primed IL-1Ra^{Mafb} and IL-1Ra^{LysM} mice contained 3- and 2-fold more neutrophils, respectively (Figures 2D, S4A, and S4B). Relative to IL-1Ra$^{fl/fl}$ controls, tissue-infiltrating neutrophils in IL-1Ra^{Mafb} and IL-1Ra^{LysM} mice exhibited substantially augmented fungicidal activity and secreted higher amounts of IL-1β, indicating their increased activation (Figures 2E and 2F). Still, deletion of IL-1Ra in CD11c-expressing cells did not affect neutrophil numbers in the blood and only slightly enhanced their peritoneal recruitment in IL-1Ra^{CD11c} mice (Figures 2C and 2D); yet, it endowed tissue-infiltrating neutrophils with enhanced fungicidal capacity, similar to that observed in IL-1Ra^{Mafb} and IL-1Ra^{LysM} mice (Figure 2E).

Characterization of neutrophil phenotypes in the blood, spleen, and kidneys revealed an enrichment of CD101^{+} neutrophils producing high levels of ROS and higher frequencies of neutrophils expressing IL-1β and MPO in the kidneys of infected IL-1Ra^{Mafb} mice compared with IL-1Ra$^{fl/fl}$ controls (Figures 2G–2J). Neutrophils in the kidneys of IL-1Ra^{LysM} and IL-1Ra^{CD11c} mice displayed intermediate phenotypes (Figures 2G–2J). CD63 expression correlated with exposure to *Candida* in infected organs, but was not influenced by IL1-Ra (Figure 2I). Removal of IL-1Ra affected neither neutrophil phenotypes nor fungal titers in the spleen (Figures 2G–2J and S5D). Thus, the absence of macrophage-produced IL-1Ra promoted the rapid recruitment of highly fungicidal neutrophils to infected kidneys.

IL-1Ra^{Mafb}, IL-1Ra^{LysM}, and, to a lesser extent, IL-1Ra^{CD11c} mice restricted fungal replication in kidneys by day 3 p.i. (Figures 1F–1H). As a result, they did not exhibit the dysfunctional hyper-inflammatory response detected in IL-1Ra$^{fl/fl}$ controls (Figures 1I–1L) and expressed lower levels of pro-inflammatory

(D) Absolute neutrophil and monocyte counts in peritoneal lavages of indicated mice at 18 h post zymosan injection.
(E and F) Fungicidal activity (E) and IL-1β secretion (F) of kidney neutrophils purified from indicated mice on day 2 p.i. (n = 6 mice/group).
(G–J) Frequencies of CD101^{+} ROS^{hi} (G), pro-IL-1β^{+} (H), CD63^{+} (I), and MPO^{+} (J) neutrophils in the blood, spleen, and kidney of indicated strains on day 2 p.i. (n = 4 mice/group, representative experiment of two).
(K and L) Characterization of renal inflammation in indicated mice on day 2 p.i. by absolute counts of leukocyte subsets (K) and cytokine concentrations (L) (n = 6 mice/group).
(M) Heatmap displaying the top 30 differentially expressed genes (DEGs) in the kidneys of indicated mice at day 2 p.i. (*Z* scores of individual mice).
(N) GSE analysis representing changes in MSigDB hallmark pathways in the kidneys of infected IL-1Ra^{Mafb} over IL-1Ra$^{fl/fl}$ mice.
(O) Key DEGs within Gene Ontology (GO) term inflammatory response in the kidneys of IL-1Ra$^{fl/fl}$ and IL-1Ra^{Mafb} mice. Mean *Z* scores, 5 mice/group.
Error bars represent mean ± SEM. *p < 0.05; **p < 0.01; ***p < 0.001; ****p < 0.0001.
See also Figures S4 and S5.

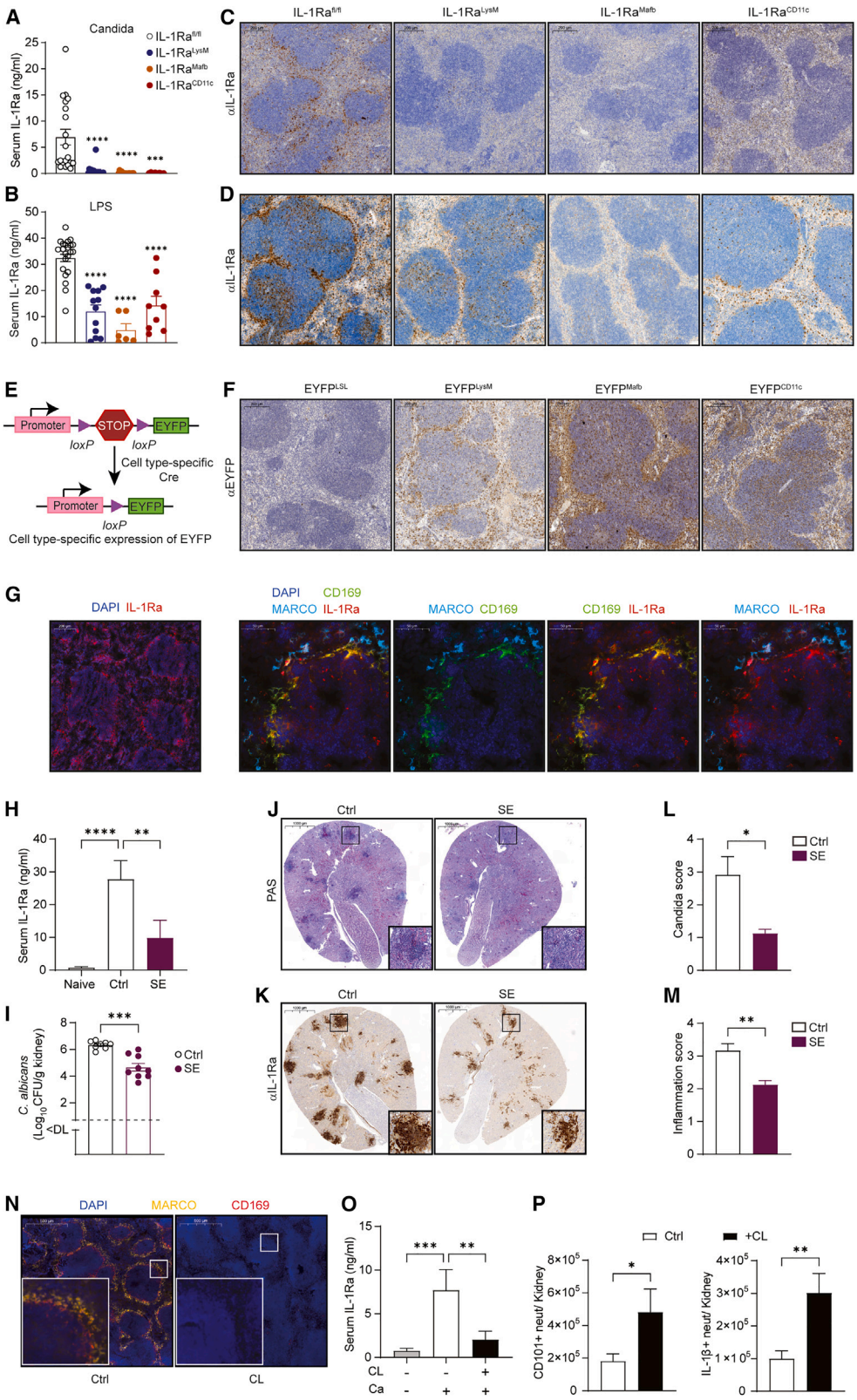

Figure 3. Serum IL-1Ra is produced by CD169$^+$ marginal zone macrophages

(A–D) IL-1Ra expression in the serum (A and B) and spleen (C and D) of indicated mice on day 3 p.i. (A and C) or 5 h post LPS injection (B and D). Scale bars, 200 μm (n = 6–15 mice/group, three experiments pooled).

(legend continued on next page)

Please cite this article in press as: Gander-Bui et al., Targeted removal of macrophage-secreted interleukin-1 receptor antagonist protects against lethal *Candida albicans* sepsis, Immunity (2023), https://doi.org/10.1016/j.immuni.2023.06.023

cytokines (Figures 2L and S4C). In addition, the kidneys of IL-1Ra^{Mafb} and IL-1Ra^{LysM} mice contained less neutrophils and inflammatory monocytes at this time, which may reflect the lower fungal burden and accelerated inflammation resolution in these mice (Figures 2K, 4D, and S5A). Bulk tissue RNA-seq of infected kidneys and gene set enrichment analysis (GSEA) associated the absence of macrophage-expressed IL-1Ra in IL-1Ra^{Mafb} mice with the suppression of inflammatory pathways including IL-6/Jak/Stat3 signaling, IFN-α response, and TNF-α signaling (Figures 2M and 2N). Besides *Il1rn*, transcripts reduced in the kidneys of IL-1Ra^{Mafb} mice included key chemoattractants *Ccl2*, *Cxcl2*, and *Cxcl1*; adhesion molecule *Icam1*; the regulator of NF-κB signaling, *Nfkbia*; and antifungal effector *Cybb* (Figures 2O, S4E, and S4F). We conclude that deletion of macrophage-specific IL-1Ra promotes rapid neutrophil-mediated pathogen elimination, which limits the detrimental hyper-inflammation triggered by sustained fungal proliferation.

Serum IL-1Ra is produced by CD169$^+$ macrophages of the splenic marginal zone

Minimal residual Cre activity in neutrophils and monocytes prompted us to address a potential cell-intrinsic function of IL-1Ra. However, partial removal of IL-1Ra in mixed BMC equally affected the recruitment and effector functions of cells originating from both, IL-1Ra-expressing and IL-1Ra gene-modified BM (Figures S6A–S6G). This suggested a cell-extrinsic effect, likely mediated by IL-1Ra secreted from macrophages. Given that these results emphasized an essential role of macrophage-secreted IL-1Ra and provided that we detected substantial levels of circulating serum IL-1Ra in infected mice (Figure 1C), we next sought to assess the impact of IL-1Ra secreted into the blood circulation and to identify the macrophage subset contributing to serum IL-1Ra production.

Bloodstream infection with *C. albicans* stimulated the release of serum IL-1Ra in wild-type mice; yet, this response was absent from IL-1Ra^{LysM}, IL-1Ra^{Mafb}, and IL-1Ra^{CD11c} mice (Figure 3A). Likewise, lipopolysaccharide (LPS) infusion elicited vigorous serum IL-1Ra production, which was considerably reduced in all conditional IL-1Ra-deficient strains tested (Figure 3B). Intravenous injection of either *Candida* or LPS induced expression of the IL-1Ra protein in the splenic marginal zone. Splenic IL-1Ra production corresponded to the presence of IL-1Ra in serum and was strongly reduced in IL-1Ra^{LysM}, IL-1Ra^{Mafb}, and IL-1Ra^{CD11c} mice primed with *Candida* or LPS (Figures 3C and 3D). EYFP expression confirmed a history of Cre activity in cells present in the marginal zone of EYFP^{LysM}, EYFP^{Mafb}, and EYFP^{CD11c} mice. Mafb-Cre-activity appeared to EYFP-mark cells in the splenic marginal zone most extensively and also affected macrophages in the red pulp (Figures 3E and 3F). This corresponded well to the efficient IL-1Ra deletion in the spleens and sera of IL-1Ra^{Mafb} mice, as well as their robust protection against invasive candidiasis. Immunofluorescence co-staining identified CD169$^+$ macrophages of the splenic marginal zone as main producers of IL-1Ra, whereas MARCO$^+$ macrophages appeared IL-1Ra negative (Figure 3G).

We directly examined the relevance of splenic IL-1Ra production for the serum IL-1Ra response and antifungal immune defense in splenectomized wild-type mice infected with *C. albicans*. Prior surgical removal of the spleen reduced the levels of *Candida*-induced serum IL-1Ra compared with mock-treated, *Candida*-infected controls (Figure 3H). Moreover, splenectomy conferred increased resistance against *Candida* replication, as indicated by reduced fungal loads (Figure 3I), restricted *Candida* dissemination and lower inflammation in kidneys (Figures 3J–3M). To verify that serum IL-1Ra was, indeed, secreted by splenic CD169$^+$ macrophages, we adopted a clodronate depletion protocol that allows selective targeting of marginal zone-resident macrophages by exploiting their distinct repopulation kinetics[35] (Figures 3N, S6H, and S6I). Depletion of splenic marginal zone macrophages and marginal metallophilic macrophages reduced serum IL-1Ra levels to that of uninfected mice (Figure 3O) and was associated with an increased recruitment of CD101$^+$ neutrophils and of IL-1β^+ neutrophils to the kidney (Figures 3P and S6J–S6M). Collectively, these findings establish a direct correlation between IL-1Ra expression in CD169$^+$ macrophages of the splenic marginal zone and the production of serum IL-1Ra following hematogenic dissemination of *C. albicans*.

Serum IL-1Ra represents an innate immune checkpoint mediating impaired pathogen control and dysfunctional hyper-inflammation during invasive fungal infection

Our findings so far revealed that macrophage-produced IL-1Ra impedes the efficient early containment of disseminated candidiasis by restricting the tissue recruitment and antifungal capacity of neutrophils. They also indicated a substantial contribution of serum IL-1Ra released from splenic CD169$^+$ macrophages. To examine the impact of circulating IL-1Ra on the immune response to *Candida*, we next reconstituted the pool of serum IL-1Ra in IL-1Ra^{Mafb} mice with intravenous infusions of the recombinant IL-1Ra protein. We reasoned that because IL-1Ra^{Mafb} mice were deficient in both circulating serum IL-1Ra and IL-1Ra produced by macrophages within infected tissues, this approach would allow to selectively investigate the contribution of serum IL-1Ra. Bolus injection of recombinant IL-1Ra raised serum IL-1Ra levels in *Candida*-infected IL-1Ra^{Mafb}

(E) Cartoon depicting EYFP-reporter used in (F).
(F) Representative EYFP-staining in the spleen of Cre-reporter mice at 5 h post LPS injection. Scale bars, 200 μm.
(G) Immunofluorescence co-staining for MARCO (cyan), CD169 (green), IL-1Ra (red), and DAPI (dark blue) in the spleen on day 2 p.i. Scale bars, 200 μm (left) and 50 μm (right).
(H–K) Analysis of splenectomized (SE) and control (ctrl) mice on day 3 p.i. for serum IL-1Ra (H), and *Candida* titers (I), PAS (J), and IL-1Ra staining (K) in the kidney. Scale bars indicate 1,000 μm (n = 8 mice/group).
(L and M) Histopathological evaluation of fungal dissemination (L) and inflammation (M) in (J) (n= 4–6 mice/group, representative experiment).
(N–Q) Analysis of clodronate liposome-treated (CL) and control (ctrl) mice on day 3 p.i. for macrophage depletion (N), serum IL-1Ra (O), and CD101$^+$ (P) and pro-IL-1β^+ (Q) neutrophils (Q) in the kidney. Scale bars, 500 μm.
Error bars represent mean ± SEM. *p <0.05; **p <0.01; ***p <0.001; ****p <0.0001.
See also Figure S6 and supplemental information.

Please cite this article in press as: Gander-Bui et al., Targeted removal of macrophage-secreted interleukin-1 receptor antagonist protects against lethal *Candida albicans* sepsis, Immunity (2023), https://doi.org/10.1016/j.immuni.2023.06.023

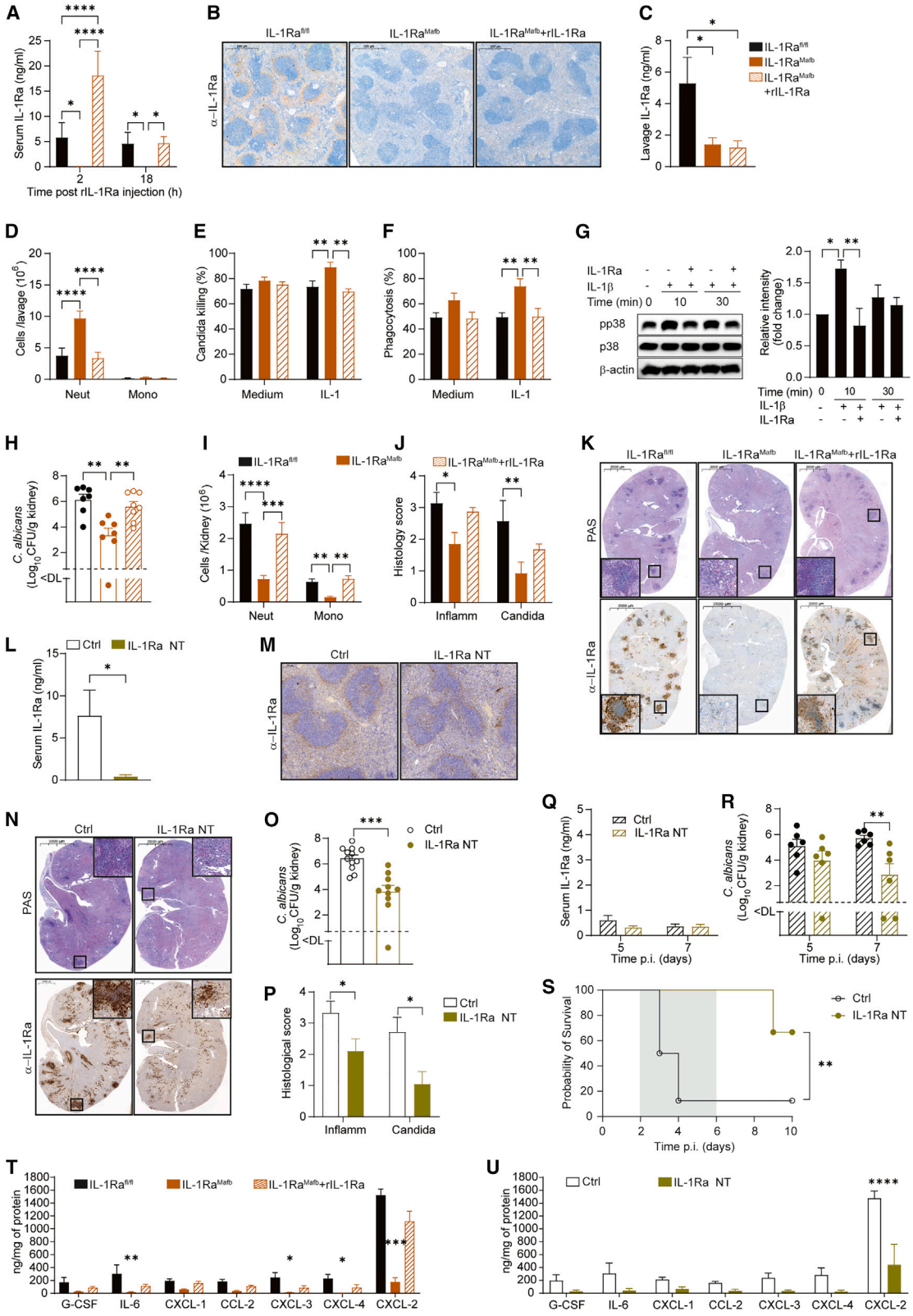

(legend on next page)

Please cite this article in press as: Gander-Bui et al., Targeted removal of macrophage-secreted interleukin-1 receptor antagonist protects against lethal *Candida albicans* sepsis, Immunity (2023), https://doi.org/10.1016/j.immuni.2023.06.023

mice initially above that of IL-1Ra competent mice but maintained wild-type levels for up to 18 h (Figures 4A and S7A). We therefore administered two daily injections throughout the experiment to fully replenish serum IL-1Ra in IL-1Ra^{Mafb} mice. The absence of IL-1Ra in the splenic marginal zone following *Candida* infection (Figure 4B) or in peritoneal exudates during zymosan peritonitis (Figure 4C) confirmed that this regimen restored exclusively serum IL-1Ra, but not the locally secreted cytokine. Reconstitution of serum IL-1Ra almost completely reverted the protected phenotype of IL-1Ra^{Mafb} mice to that of IL-1Ra$^{fl/fl}$ controls. For example, the enhanced neutrophil recruitment to zymosan priming observed in IL-1Ra^{Mafb} mice was abrogated upon replenishing their serum IL-1Ra (Figure 4D). Likewise, reconstitution of serum IL-1Ra restricted the fungicidal and phagocytic activities of neutrophils in IL-1Ra^{Mafb} mice to the level of IL-1Ra-competent wild-type mice. Moreover, the *ex vivo* effector functions of neutrophils from IL-1Ra^{Mafb} mice but not from IL-1Ra-reconstituted IL-1Ra^{Mafb} mice were amplified by *in vitro* IL-1β stimulation, suggesting that the absence of serum IL-1Ra *in vivo* increased the sensitivity of neutrophils to local IL-1β stimulation (Figures 4E and 4F). Indeed, when primary neutrophils were pre-pulsed with IL-1Ra *in vitro*, this abolished their IL-1R signaling upon subsequent exposure to IL-1β even after removal of unbound extracellular IL-1Ra (Figure 4G). As could be expected from these results, IL-1Ra-reconstituted IL-1Ra^{Mafb} mice no longer controlled *Candida* replication in their kidneys as efficiently as IL-1Ra^{Mafb} mice. Instead, they presented with higher fungal loads, increased *Candida* dissemination and stronger renal inflammation (Figures 4H–4K); thus, they displayed a phenotype similar to that of IL-1Ra$^{fl/fl}$ controls. This showed that the pronounced immediate resistance of IL-1Ra^{Mafb} mice to *Candida* was mainly attributable to the lack of serum IL-1Ra in these mice and emphasized the impact of serum IL-1Ra on the early immune control of *C. albicans*. In addition, it suggested that targeted removal of IL-1Ra might provide a valid strategy to harness the endogenous antifungal response during disseminated candidiasis.

We therefore tested whether *in vivo* neutralization of IL-1Ra prior to infection increased the ability of wild-type mice to contain fungal infection (Figure S7B). Daily injections of a neutralizing antibody against murine IL-1Ra[36] efficiently depleted serum IL-1Ra; yet, it did not affect IL-1Ra protein expression in the splenic marginal zone (Figures 4L and 4M). Furthermore, preventive IL-1Ra neutralization greatly improved the immune control of *Candida* infection, as illustrated by reduced fungal titers, limited *Candida* dissemination, and lower tissue inflammation in infected kidneys (Figures 4N–4P). We observed that serum concentrations of IL-1Ra peaked on day 2 p.i. and returned to naive levels by day 7 p.i. (Figures 1C and 4Q). We hence scrutinized whether therapeutic IL-1Ra neutralization protected against lethal *C. albicans* infection (Figure S7C). Indeed, IL-1Ra neutralization with onset at day 2 p.i. reduced fungal titers and markedly enhanced the survival of wild-type mice upon high dose *C. albicans* challenge (Figures 4Q–4S). The phenotypes of IL-1Ra^{LysM}, IL-1Ra^{Mafb}, and IL-1Ra^{CD11c} mice already revealed that an early suppression of fungal replication prevented the dysfunctional inflammatory response observed in wild-type IL-1Ra$^{fl/fl}$ controls (Figure 2L). These observations were confirmed following the depletion and reconstitution of serum IL-1Ra. Whereas IL-1Ra^{Mafb} mice displayed very low pro-inflammatory cytokine levels in the kidney, reconstitution of serum IL-1Ra in these mice not only hampered their ability to restrict *Candida* proliferation (Figure 4H) but also caused renal hyper-inflammation similar to that seen in IL-1Ra$^{fl/fl}$ mice (Figures 4T and S7E). Conversely, neutralization of IL-1Ra promoted the rapid immune control of *Candida* in wild-type mice and was associated with greatly reduced inflammatory profiles in their kidneys (Figures 4O, 4U, and S7F). These data directly link macrophage-produced IL-1Ra to the ineffective immune control of invasive fungal infection and the resulting dysfunctional inflammatory response and thereby suggest serum IL-1Ra as a biomarker and potential therapeutic target for disseminated candidiasis.

IL-1Ra secreted by infiltrating macrophages limits pathogen elimination in infected tissue

Our findings demonstrate the significant impact of serum IL-1Ra on the immune defense against *Candida*. Nevertheless, the transient protection observed in IL-1Ra^{CD11c} mice indicated that later stages of the response were influenced by IL-1Ra secreted from a second macrophage population sensitive to gene deletion mediated by Mafb-Cre but not CD11c-Cre. We therefore

Figure 4. Serum IL-1Ra mediates the impaired pathogen control and dysfunctional hyper-inflammation during disseminated *Candida* infection

(A–C) Analysis of IL-1Ra reconstitution in IL-1Ra^{Mafb} mice in the serum (A) and spleen (B) during *Candida* infection and in peritoneal lavage (C) during zymosan-induced peritonitis (A, n = 7 mice/group; C, n = 9 mice/group). Scale bars, 200 μm.

(D–F) Characterization of peritoneal infiltrates of IL-1Ra-reconstituted IL-1Ra^{Mafb} mice at 18 h post i.p. zymosan by absolute counts (D), fungicidal neutrophil activity (E), and phagocytosis (F) (n = 6 mice/group, two pooled experiments).

(G) Western blot analysis of IL-1R-signaling in neutrophils with or without prior IL-1Ra pulse treatment.

(H, I, and K) Characterization of IL-1Ra-reconstituted mice at day 3 p.i. by fungal titers (H), cellular infiltrates (I), PAS and IL-1Ra staining (K) in the kidney. Scale bars, 2,000 μm. (n = 7 mice/group, two pooled experiments).

(J) Histopathological quantification of fungal replication and inflammation in (K).

(L–P) Preventive IL-1Ra neutralization (NT) at day 3 post *Candida* infection examined by IL-1Ra expression in the serum (L) and spleen (M), PAS and IL-1Ra staining (N), and fungal kidney titers (O). Scale bars, 200 μm in (M), 1,000 μm in (N) (bottom), and 2,000 μm (N) (top).

(P) Histopathological quantification of *Candida* replication and inflammation in (N) (n = 6–10 mice/group, three pooled experiments).

(Q–S) Therapeutic IL-1Ra neutralization in *Candida*-infected wild-type mice assessed by serum IL-1Ra (Q), renal *Candida* titers (R), and survival probability (S) (n = 6–7 mice/group, two pooled experiments).

(T and U) Inflammatory profiles in the kidneys of indicated mice following reconstitution (T) or neutralization (U) of IL-1Ra as determined by cytokine array (n = 5–7 mice/group).

Error bars represent mean ± SEM. *p < 0.05; **p < 0.01; ***p < 0.001; ****p < 0.0001.

See also Figure S7.

Please cite this article in press as: Gander-Bui et al., Targeted removal of macrophage-secreted interleukin-1 receptor antagonist protects against lethal *Candida albicans* sepsis, Immunity (2023), https://doi.org/10.1016/j.immuni.2023.06.023

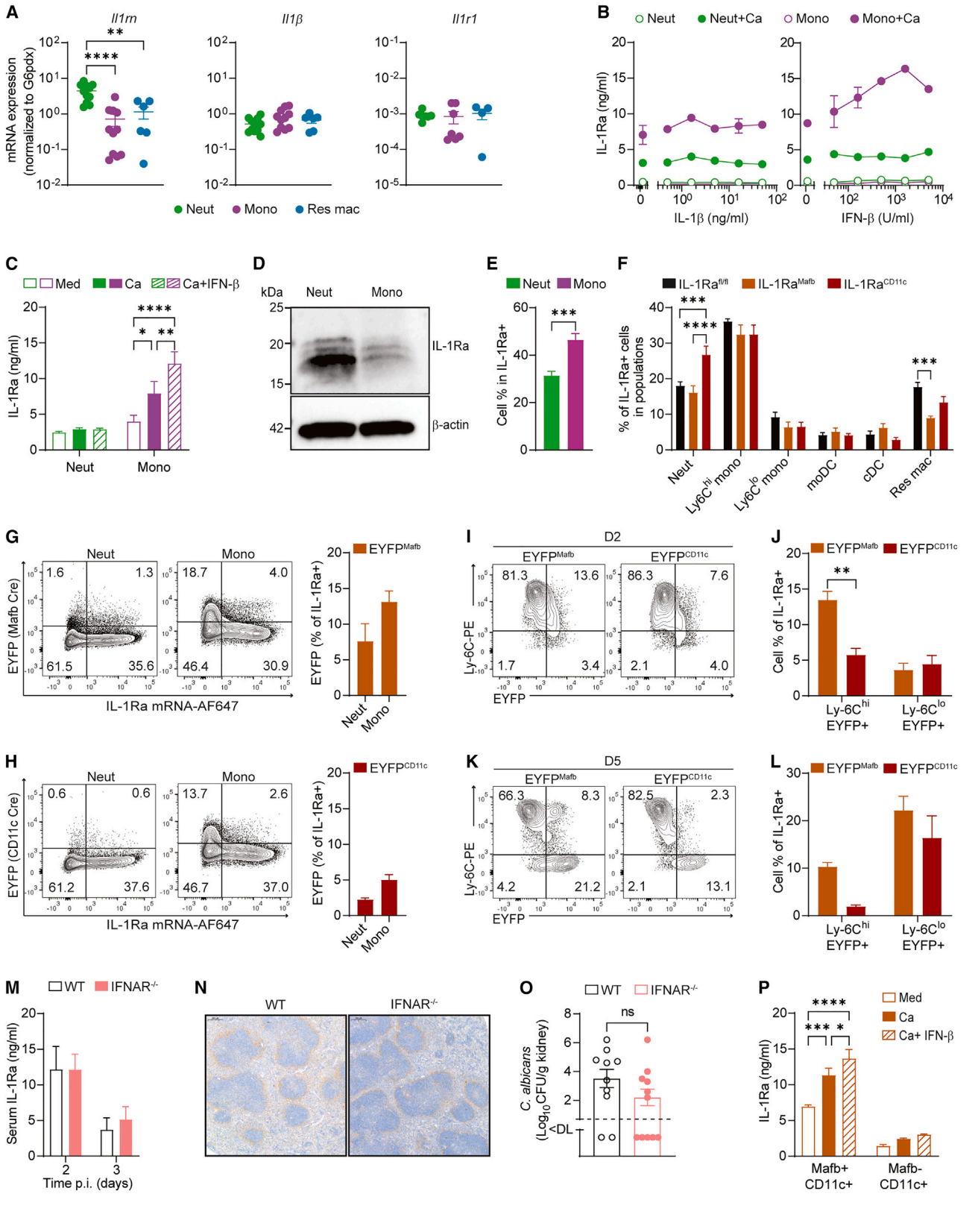

(legend on next page)

Please cite this article in press as: Gander-Bui et al., Targeted removal of macrophage-secreted interleukin-1 receptor antagonist protects against lethal *Candida albicans* sepsis, Immunity (2023), https://doi.org/10.1016/j.immuni.2023.06.023

interrogated the relevance of IL-1Ra produced locally in infected tissues and characterized the IL-1Ra-responses of kidney-infiltrating leukocytes. Neutrophils, inflammatory monocytes, and kidney-resident macrophages comprised the main leukocyte populations present in kidneys on day 3 p.i. (Figure 2K). Analysis of fluorescence-activated cell sorting (FACS)-purified cells from infected mice revealed highest mRNA expression of IL-1Ra in neutrophils, whereas all three populations expressed IL-1β and IL-1R1 at comparable levels (Figure 5A). Still, exposure of naive primary cells to *Candida in vitro* provoked much stronger IL-1Ra protein secretion from monocytes than from neutrophils. Simultaneous IL-1β cytokine stimulation affected IL-1Ra secretion of neither monocytes nor neutrophils (Figure 5B). However, we found that type I IFN markedly augmented the *Candida*-elicited IL-1Ra secretion in monocytes; yet, it did not affect IL-1Ra release from neutrophils (Figure 5B). Likewise, neutrophils isolated from infected kidneys secreted low levels of IL-1Ra irrespective of *ex vivo* exposure to *Candida* or type I IFN (Figure 5C). In contrast, inflammatory monocytes isolated from the same animals released substantial amounts of IL-1Ra in response to *Candida*, which were further augmented by additional IFN-β stimulation (Figure 5C). Western blot analysis revealed that neutrophils predominantly expressed the 16 kDa intracellular isoform of IL-1Ra, which may explain the discrepant mRNA expression and cytokine secretion detected for these cells in response to *Candida* (Figure 5D). Taken together, these data identified inflammatory monocytes as main early IL-1Ra producers in infected tissue and suggested the positive regulation of their response by type I IFN.

Intracellular mRNA staining by Prime Flow analysis confirmed that inflammatory monocytes represented more than 50% of total IL-1Ra mRNA-positive leukocytes on day 2 p.i. (Figure 5E). However, a contribution of monocyte-secreted IL-1Ra to the enhanced protection seen in IL-1Ra^{Mafb} or IL-1Ra^{CD11c} mice seemed unlikely, as both strains contained wild-type proportions of IL-1Ra mRNA-positive monocytes (Figure 5F) and given that EYFP^{Mafb} and EYFP^{CD11c} reporter mice displayed negligible Cre activity in kidney-infiltrating monocytes (Figures 5G, 5H, and S7G). Nevertheless, we observed the appearance of a second Ly-6C^{lo} MHC II^{+} F4/80^{+} IL-1Ra-producing population, presumably monocyte-derived macrophages, which comprised 40% of IL-1Ra producers by day 5 p.i. (Figures 5I–5L and S7H). This subset exhibited higher Cre activity in EYFP^{Mafb} than in EYFP^{CD11c} reporter mice, suggesting that IL-1Ra would be more efficiently deleted in these cells in IL-1Ra^{Mafb} mice (Figures 5K and 5L). Provided that type I IFN augmented IL-1Ra secretion from monocytes, we examined its impact on the macrophage-produced IL-1Ra response. Type I IFN was not required to induce serum IL-1Ra in response to *Candida* infection, as mice deficient in type I IFN-α/β receptor (IFNAR) signaling (IFNAR$^{-/-}$)[37] showed wild-type IL-1Ra expression in the spleen and serum (Figures 5M and 5N) and controlled fungal replication in kidney equally well as controls (Figures 5O and S7I). Type I IFN preferentially boosted IL-1Ra secretion in the subset of MafbCre-marked monocyte-derived macrophages, which we had identified as key IL-1Ra producers (Figure 5K). In particular, among all CD11c^{+} macrophages isolated from infected kidneys of EYFP^{Mafb} mice on day 5 p.i., only the EYFP^{+} MafbCre-marked population showed substantial IL-1Ra secretion in response to *Candida*, which was amplified by concomitant IFN-β stimulation (Figure 5P). In summary, these results highlight the impact of IL-1Ra secreted by monocyte-derived macrophages in infected tissue. Moreover, they suggest that the particularly efficient gene targeting of this type I IFN-sensitive population in IL-1Ra^{Mafb} mice contributes to their sustained long-term protection against *Candida*.

Type I IFN amplifies the macrophage IL-1Ra response and exacerbates fungal sepsis

Prior viremia can predispose hospitalized patients to secondary invasive fungal infections,[12] and our data demonstrated that type I IFN signaling potentiates the *Candida*-induced IL-1Ra secretion from macrophages; therefore, we evaluated whether IFN-I responses elicited in context of viral infection could induce IL-1Ra as a permissive factor for subsequent invasive candidiasis. Intravenous injection of IFN-β confirmed its ability to directly elicit a serum IL-1Ra response (Figure 6A). Moreover, i.v. administration of the synthetic TLR3 agonist polyinosinic-polycytidylic acid (PIC)—a well-established method to induce robust IFN-I production in mice—rapidly triggered expression of IL-1Ra mRNA and protein in the spleen and induced substantial levels of circulating IL-1Ra in the serum (Figures 6B–6D). However, PIC elicited no such IL-1Ra production in IL-1Ra^{Mafb} mice, suggesting that fungal infection and IFN-I stimulated the identical

Figure 5. IL-1Ra from infiltrating macrophages limits pathogen elimination in infected tissue

(A) mRNA expression of IL-1 family genes in indicated cell subsets on day 2 p.i.

(B and C) IL-1Ra production by neutrophils and monocytes stimulated with *Candida* in the presence or absence of IL-1β or IFN-β *in vitro*. Cells were purified from naive mice (B) or on day 2 p.i. (C) (B, duplicate cultures, n = 4 mice; C, n = 4–7 mice).

(D) Western blot analysis of IL-1Ra isoforms in *Candida*-stimulated neutrophils and monocytes.

(E) Frequencies of neutrophils and monocytes among IL-1Ra mRNA-expressing kidney leukocytes at day 2 p.i. (n = 7 mice/group, two pooled experiments).

(F) Frequencies of IL-1Ra mRNA-expressing cells within indicated immune cell subsets of IL-1Ra$^{fl/fl}$, IL-1Ra^{Mafb}, and IL-1Ra^{CD11c} mice at day 2 p.i. (n = 7 mice/group, two experiments).

(G–L) Analysis of Cre-expression in IL-1Ra mRNA-expressing leukocytes of EYFP^{Mafb} and EYFP^{CD11c} mice on days 2 (G–J) and 5 (K and L) p.i. Expression of EYFP and IL-1Ra mRNA in neutrophils or monocytes from EYFP^{Mafb} (G) and EYFP^{CD11c} (H) mice assessed by flow cytometry and quantification (n = 4–8 mice/group).

(I–L) Frequency of EYFP expression among IL-1Ra mRNA-expressing Ly6G^{-} CD11b^{+} cells of EYFP^{Mafb} and EYFP^{CD11c} mice at days 2 (I and J) and 5 (K and L) p.i. (n = 4–8 mice/group).

(M–O) Characterization of IFNAR$^{-/-}$ mice by IL-1Ra expression in serum (M) and spleen (N), and fungal burden in kidney (O) on day 3 p.i. (n= 4–8 mice/group). Scale bars, 200 μm.

(P) IL-1Ra production by EYFP^{Mafb} macrophages FACS-purified *ex vivo* on day 5 p.i. and stimulated *in vitro* as indicated (n = 6 mice/group, two pooled experiments).

Error bars represent mean ± SEM. *p < 0.05; **p < 0.01; ***p < 0.001; ****p < 0.0001.

See also Figure S7.

Please cite this article in press as: Gander-Bui et al., Targeted removal of macrophage-secreted interleukin-1 receptor antagonist protects against lethal *Candida albicans* sepsis, Immunity (2023), https://doi.org/10.1016/j.immuni.2023.06.023

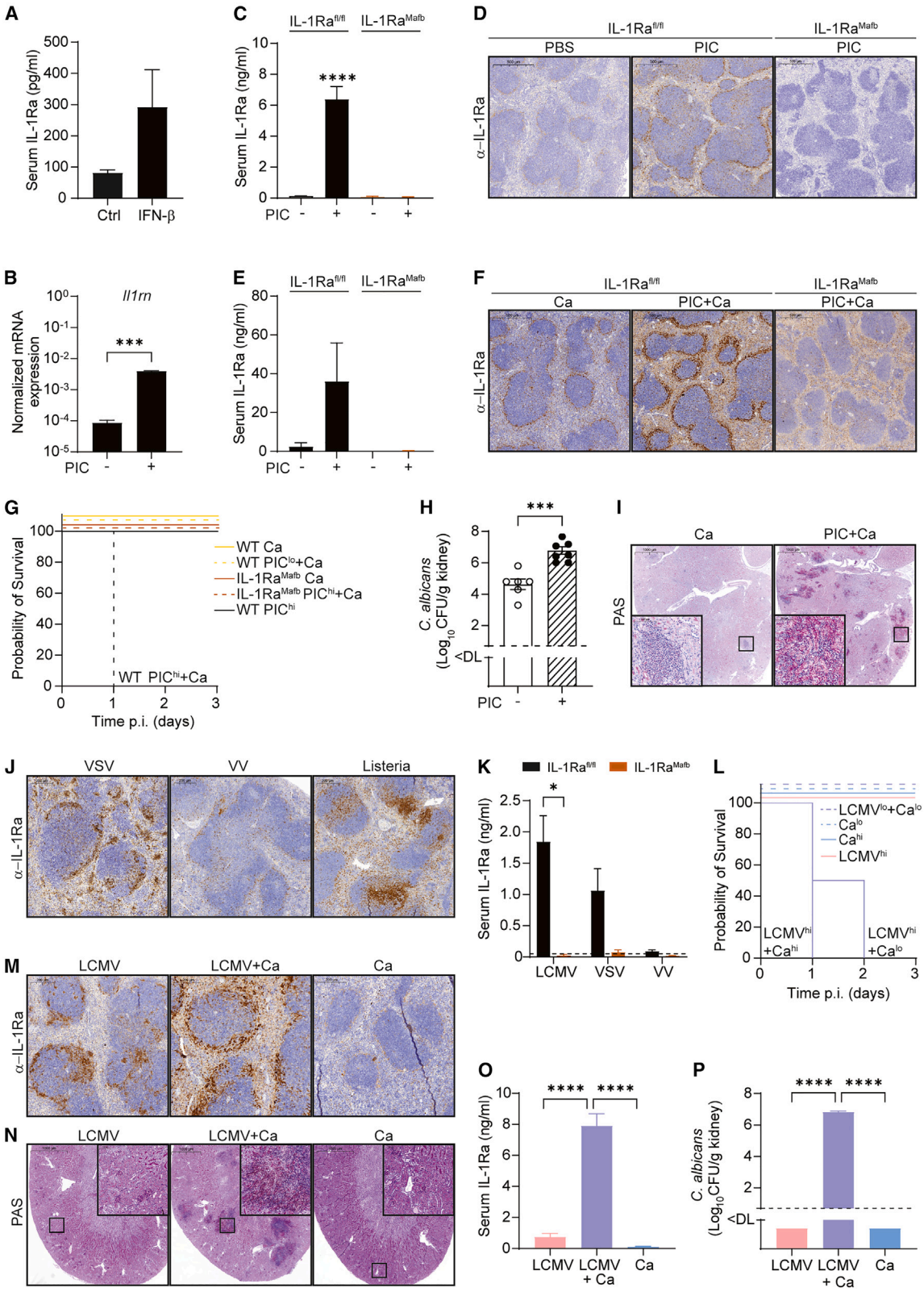

Figure 6. Type I IFN amplifies the macrophage IL-1Ra response and exacerbates fungal sepsis

(A and B) *In vivo* induction of IL-1Ra by type I IFN as evaluated by serum IL-1Ra (A) and kidney mRNA expression (B) following injection of IFN-β or PIC, respectively (n = 7 mice/group, two pooled experiments).

(legend continued on next page)

Please cite this article in press as: Gander-Bui et al., Targeted removal of macrophage-secreted interleukin-1 receptor antagonist protects against lethal *Candida albicans* sepsis, Immunity (2023), https://doi.org/10.1016/j.immuni.2023.06.023

macrophage population to release IL-1Ra (Figures 3A, 3C, 6C, and 6D). Moreover, PIC treatment considerably amplified the *Candida*-induced IL-1Ra response in the spleen and serum (Figures 6E and 6F) and as a result rendered mice highly susceptible to fungal infection. In particular, PIC-treated mice showed greatly increased morbidity upon infection with 2.5×10^5 CFU *Candida* and had to be prematurely removed from the experiment, whereas this fungal dose was tolerated in the absence of PIC-induced IFN-I (Figure 6G). In contrast, PIC-elicited IFN-I failed to trigger detectable IL-1Ra production and did not aggravate disease severity in *Candida*-infected IL-1Ra^{Mafb} mice (Figures 6F and 6G). This confirmed the IFN-driven amplification of macrophage-produced IL-1Ra as underlying mechanism for the enhanced susceptibility to *Candida* infection following PIC injection in wild-type mice. Co-injection of PIC also exacerbated the disease severity in IL-1Ra$^{+/+}$ mice upon infection with a lower *Candida* inoculum (Figures 6H and 6I). Whereas we detected minimal levels of serum IL-1Ra in mice receiving 10^5 CFU *Candida* alone, the simultaneous induction of IFN-I strongly augmented the serum IL-1Ra response, interfered with the early immune control of *C. albicans* and increased fungal titers in the kidney by two orders of magnitude (Figures 6H and 6I). Confirming these observations, infection with microbial pathogens known to stimulate IFN-I production *in vivo*, such as lymphocytic choriomeningitis virus (LCMV), vesicular stomatitis virus (VSV), vaccinia virus (VV), or *Listeria monocytogenes*, triggered IL-1Ra expression in the spleen, albeit to different degrees (Figures 6J and 6M). In particular, the potent IFN-I inducers LCMV and VSV elicited strong serum IL-1Ra production from MafbCre-marked macrophages (Figure 6K).

LCMV represents a well-characterized experimental model that recapitulates relevant aspects of systemic viral infection in human patients; therefore, we further interrogated the impact of IFN-augmented IL-1Ra production on susceptibility to fungal bloodstream dissemination in the context of LCMV-WE infection. Similar to our findings with PIC-induced IFN-I, a high dose LCMV co-infection massively exacerbated the morbidity of *Candida*-infected mice, and fungal doses tolerated in control mice without LCMV co-infection were no longer contained and caused exacerbated morbidity (Figure 6L). Although low dose LCMV-infected mice were able to control a lower *Candida* inoculum (10^5 CFU) until day 3 p.i., they nevertheless exhibited very high levels of serum IL-1Ra (Figure 6O) and showed uncontrolled fungal dissemination in their kidneys (Figures 6N and 6P). The aggravating effect of viral infection was strictly type-I IFN dependent, as co-infected IFNAR-deficient mice completely lacked the increased IL-1Ra responses in the spleen and serum, and their fungal titers that were comparable with those of mice infected with *C. albicans* alone (Figures 7A–7C). Accordingly, the kidneys of co-infected IFNAR-deficient mice contained isolated infectious foci and thereby resembled those of singly *C. albicans*-infected controls, whereas the kidneys of co-infected wild-type mice displayed unrestricted fungal dissemination (Figure 7A). Transcripts of IFN-regulated genes *Ifit1*, *Isg15*, and *Mx1* revealed that *C. albicans* infection per se triggered considerable IFNAR signaling in the spleen and kidney, which was further enhanced by virally induced IFN-I (Figures 7D and 7E). Still, the *Il1rn* expression in context of *C. albicans* infection appeared to be IFN independent, whereas its viral amplification was partially IFNAR dependent (Figures 7D and 7E). Co-infection of IL-1Ra^{Mafb} mice confirmed that LCMV-induced IFNAR signaling elicited serum IL-1Ra production from MafbCre-marked macrophages (Figure 7F). Furthermore, it revealed that virally induced IFN-I exacerbated *Candida* infection in part by amplifying the macrophage-produced IL-1Ra response but also through IFNAR-dependent mechanisms unrelated to macrophage-produced IL-1Ra (Figure 7G). Altogether, these observations demonstrate that type I IFN elicited during viral infection strongly increases the susceptibility to *Candida* bloodstream infection with detrimental consequences for host survival and implicate macrophage-produced IL-1Ra in this process.

DISCUSSION

Due to the high disease-related mortality and limited treatment options, invasive fungal infections remain an urgent and inadequately addressed medical problem.[2,4,5] Our study uncovers a disease mechanism that contributes to the high disease susceptibility of disseminated candidiasis and its known amplification by viral co-infections. We identify macrophage-produced serum IL-1Ra as a disease-promoting innate immune checkpoint that can be inhibited to protect against fatal *C. albicans* sepsis in the mouse model. These findings are of immediate importance to our understanding of the pathogenesis of invasive fungal infections and may open new avenues for their treatment.

Our results emphasize the critical role of serum IL-1Ra during invasive candidiasis. Hepatocyte-produced serum IL-1Ra has been described in various inflammatory conditions.[21] In contrast, we identify splenic CD169$^+$ macrophages as main producers of serum IL-1Ra during fungal infection. Although serum IL-1Ra may be beneficial by preventing excessive IL-1 signaling in bacterial sepsis, we find that it is deleterious during invasive candidiasis. Genetic ablation of macrophage-produced IL-1Ra and liposomal depletion of marginal macrophages blunted serum IL-1Ra levels and enhanced protective neutrophil responses, thereby highlighting the impact of CD169$^+$ macrophage-derived IL-1Ra. Marginal zone macrophages sense blood-borne pathogens, including *Candida*, to instruct the

(C–F) PIC-induced IL-1Ra expression in serum (C and E) and spleen (D and F) of IL-1Ra$^{fl/fl}$ and IL-1Ra^{Mafb} mice determined 5 h post-PIC injection (C and D) or 48 h after additional *Candida* infection (E and F). Scale bars, 500 μm (C, n = 4–7; B, n = 3; E, n = 3–6 mice/group).
(G) Survival probability of IL-1Ra$^{fl/fl}$ and IL-1Ra^{Mafb} mice injected with *Candida* and PIC as indicated (n = 6 mice/group, two pooled experiments).
(H and I) Fungal burden (H) and PAS staining (I) in the kidneys of mice treated as in (G) evaluated on day 2 p.i. Scale bars, 1,000 μm. (n = 6 mice/group).
(J and M) IL-1Ra staining in the spleen at 24 h p.i. with indicated pathogens. Scale bars, 200 μm.
(K) Serum IL-1Ra levels of IL-1Ra$^{fl/fl}$ and IL-1Ra^{Mafb} mice infected as in (J) and (M). Dashed line indicates naive baseline (n = 3–7 mice/group, single experiment).
(L) Survival probability of indicated groups of infected mice (n = 4 mice/group).
(M–P) Characterization of co-infected mice at day 3 p.i. by IL-1Ra expression in spleen (M) and serum (O), PAS staining in kidney (N), and *Candida* titers in kidney (P). Scale bars, 200 μm (n = 4 mice/group, representative experiment).
Error bars represent mean ± SEM. *p < 0.05; ***p < 0.001; ****p < 0.0001.

Please cite this article in press as: Gander-Bui et al., Targeted removal of macrophage-secreted interleukin-1 receptor antagonist protects against lethal *Candida albicans* sepsis, Immunity (2023), https://doi.org/10.1016/j.immuni.2023.06.023

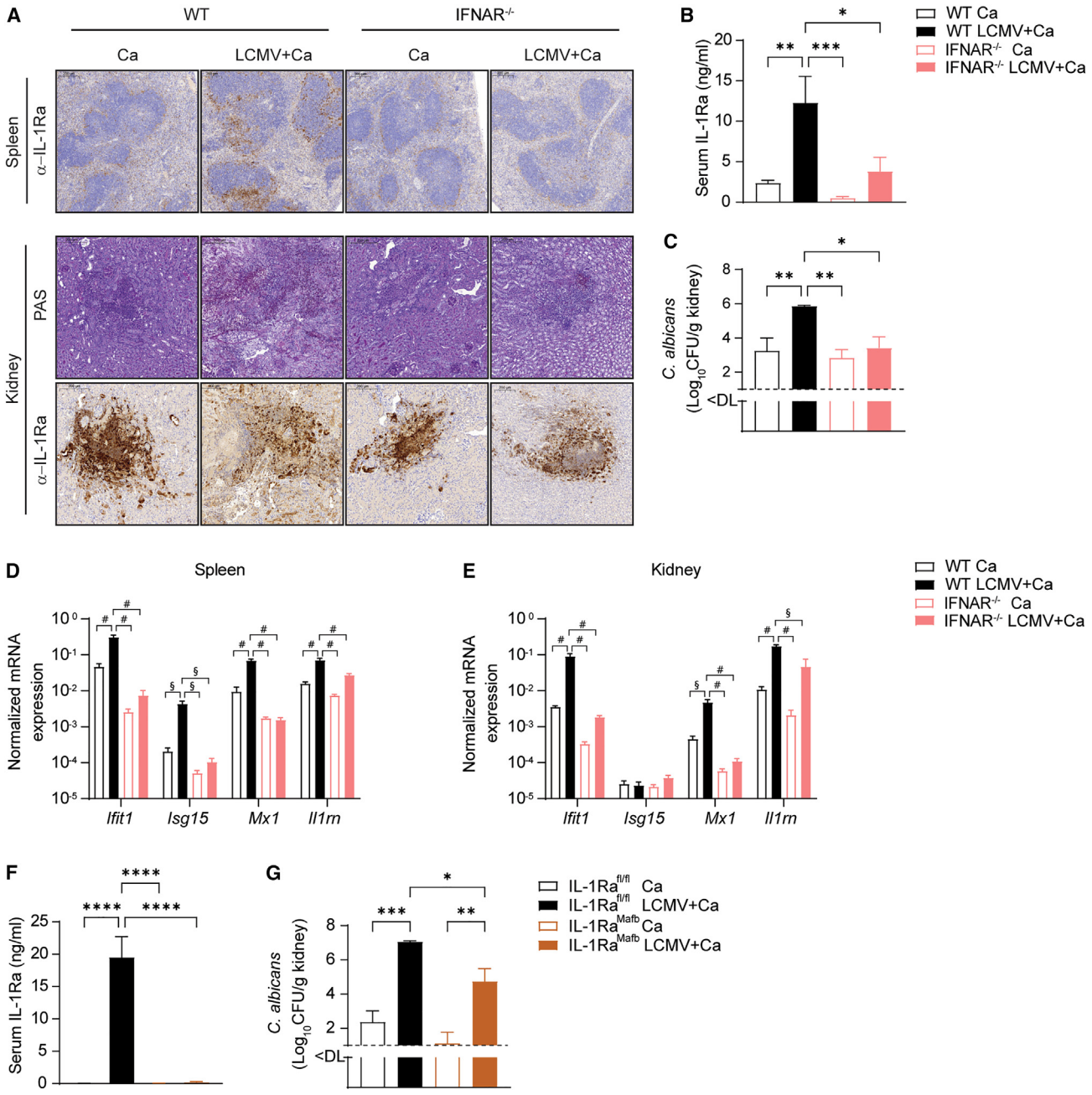

Figure 7. Virus-induced exacerbation of fungal dissemination critically depends on type I IFN and macrophage-produced IL-1Ra

(A–E) IFNAR$^{-/-}$ and wild-type mice infected with *Candida* (Ca) or co-infected with LCMV and *Candida* (LCMV + Ca) were analyzed by PAS and IL-1Ra staining of the spleen and kidney (A), serum IL-1Ra (B), fungal kidney titers (C), and mRNA expression of IFN-stimulated genes in the spleen (D) and kidney (E) on day 3 p.i. (n = 5–7 mice/group, two pooled experiments). Scale bars, 200 μm.

(F and G) Serum IL-1Ra levels (F) and kidney *Candida* titers (G) of IL-1Ra$^{fl/fl}$ and IL-1Ra^{Mafb} mice infected as in (A)–(E) (n = 4–5 mice/group, single experiment). Error bars represent mean ± SEM. *p < 0.05; **p < 0.01; ***p < 0.001; ****p < 0.0001; §p < 0.001; #p < 0.0001.

induction of innate and adaptive immunity. G-CSF released by CD169^{+} macrophages upon splenic colonization promotes neutrophil dysfunction in fungal sepsis.[38] We detected no effects on splenic neutrophils in IL-1Ra-deficient mice (Figures 2G–2J and S5A) but could modulate neutrophil functionality and renal hyper-inflammation by reconstituting or neutralizing IL-1Ra. This suggests CD169^{+} macrophage-derived IL-1Ra inhibits antifungal immunity by restricting the IL-1-driven maturation and rapid tissue recruitment of highly fungicidal neutrophils (Figures 2 and S5A). We detected a second wave of IL-1Ra produced by macrophages in infected tissue, and efficient targeting of this population may contribute to the superior resistance of IL-1Ra^{Mafb} mice to *Candida*. Besides macrophages, kidney-infiltrating neutrophils and monocytes exhibited

Please cite this article in press as: Gander-Bui et al., Targeted removal of macrophage-secreted interleukin-1 receptor antagonist protects against lethal *Candida albicans* sepsis, Immunity (2023), https://doi.org/10.1016/j.immuni.2023.06.023

considerable IL-1Ra expression, whereas that of dendritic cells or kidney-resident macrophages appeared negligible. Neutrophils contained mainly an intracellular IL-1Ra isoform and secreted limited amounts of IL-1Ra *in vitro*. This suggests that neutrophil-expressed IL-1Ra is predominantly biologically active following its release upon neutrophil death. Unlike neutrophils, monocytes secreted substantial quantities of IL-1Ra, which were further augmented by IFN-I stimulation. The Cre drivers used here did not delete IL-1Ra in monocytes (Figure 5), and we cannot conclude to which extent monocyte-secreted IL-1Ra impacts the immune defense against disseminated *Candida*. However, the fact that we observed the strong protective effect of removing macrophage-expressed IL-1Ra despite the presence of monocyte-expressed IL-1Ra argues for a predominant role of macrophage-secreted IL-1Ra.

Our study identified neutrophils as key defense mechanism regulated by macrophage-secreted IL-1Ra and demonstrated that the enhanced maturation, tissue recruitment, and functionality of neutrophils mediate the protective effect of IL-1Ra removal. Neutrophil effector pathways including phagocytosis, ROS production, and NET formation are indispensable for systemic antifungal immunity.[10,39] Our data suggest that the exposure of neutrophils to IL-1Ra in the blood determines their IL-1β responsiveness following recruitment to inflamed tissue (Figure 4). IL-1 programs neutrophil clustering behavior and their execution of defense mechanisms during antifungal responses.[40] Hence, the higher sensitivity to IL-1β stimulation (Figure 4) and increased IL-1β production (Figure 2) observed for neutrophils in the absence of IL-1Ra may enhance such neutrophil-directed activities of IL-1 and very likely also increased IL-1 signaling in other cell types, including endothelial cells, added to the superior neutrophil responses in IL-1Ra^{Mafb} mice. Enhanced IL-1 signaling may also protect against *C. albicans* by promoting granulopoiesis and via neutrophil-independent mechanisms.[41,42]

We found that macrophage-secreted IL-1Ra was positively regulated by IFN-I. Type I IFN signaling has been linked to the host defense against *Candida* in human patients.[43] However, its role in protective immunity remains controversial because both positive and negative disease outcomes were reported in IFNAR-deficient mice.[44,45] We observed no significant effects of IFNAR deficiency on *Candida* monoinfection, which might signal differences in genetic backgrounds or microbiota composition between these studies. *Candida* stimulates IFN-I secretion from conventional dendritic cells, which increases their fungicidal capacity and licenses monocytes to promote protective natural killer (NK) cell and neutrophil responses.[45–47] Conversely, type I IFN may aggravate the severity of *Candida* infection by inhibiting inflammasome activation and generation of bioactive IL-1 and by promoting hyper-inflammatory renal injury.[44–48] In addition, IFN-induced factor IFIT2 limits the ROS production and fungicidal activity of leukocytes.[49] We demonstrate that IFN-I inhibits protective IL1-signaling by augmenting IL-1Ra secretion from macrophages (Figures 6 and 7). This implicates IL-1Ra in the reciprocal crosstalk between type I IFN-driven and IL-1-driven inflammation in invasive candidiasis, as proposed for bacterial infections.[50–53] *Candida* elicited IFNAR-independent IL-1Ra production; yet, additional IFN-I signaling severely amplified the *Candida*-induced IL-1Ra response. IFN-I is induced by numerous pathogens[54] and prior viremia constitutes a risk factor for invasive candidiasis.[11,12] We show that viral co-infection drastically aggravated the disease mortality via the IFN-dependent augmentation of IL-1Ra production in Mafb-Cre-marked macrophages, which provides a potential disease mechanism for secondary candidiasis or polymicrobial sepsis. Targeting IL-1Ra in such IFN-I/IL-1 crosstalk might prove advantageous because it would enhance protective IL-1R signaling by increasing the potency of physiologically secreted, endogenous IL-1 without hindering beneficial defense mechanisms induced through type I IFN.

Although our findings establish the efficacy of IL-1Ra neutralization in the animal model, these observations should not be extrapolated to human patients without considering potential adverse effects of excessive IL-1-signaling. IL-1-mediated inflammation is absolutely essential to control *Candida* bloodstream infection, as is unequivocally shown by the fact that defects throughout the IL-1 pathway drastically increase the disease mortality.[16–18,55–58] Yet, lack of physiological balancing of IL-1 by the IL-1Ra due to genetic deficiency[23] or neutralizing anti-IL1Ra autoantibodies[59,60] results in uncontrolled IL-1-signaling and a multi-organ inflammatory syndrome. An impaired IL-1/IL-1Ra balance has been linked to hyper-inflammatory states,[19,61,62] and anakinra is considered for bacterial sepsis.[63] In contrast, we did not observe exacerbated multi-organ inflammation in IL-1Ra-deficient IL-1Ra^{Mafb} mice or following IL-1Ra neutralization during *Candida* infection. Instead, removal of IL-1Ra not only resulted in faster pathogen clearance but, surprisingly, also in the rapid and paradoxical attenuation of the pathogenic hyper-inflammation observed in mice expressing functional IL-1Ra. Accordingly, the dysfunctional inflammatory response during *Candida* sepsis is not caused by excessive IL-1 signaling, but by a failure to eliminate the pathogen. Therapeutic neutralization substantially improved the survival of wild-type mice, which should encourage the development of more efficient IL-1Ra-targeted approaches. We presume that enhancing IL-1-driven mechanisms by neutralizing IL-1Ra could be beneficial in patients with active fungal replication, but it might not be suitable for inflammatory conditions triggered by residual fungal antigen. For example, IL-1α-elicited neutrophilic inflammation is required for clearance of pulmonary Aspergillus infection, but it worsens disease outcomes in Aspergillus-induced asthma.[64,65] Thus, increased neutrophil recruitment following IL-1Ra neutralization could promote resistance to invasive fungal infection, but it may also sustain pathogenic inflammation to non-replicating fungal components.[65] Whether such mechanisms contribute to the immune reconstitution inflammatory syndrome (IRIS) in chronic disseminated candidiasis remains to be investigated.[66,67]

In conclusion, by ablating the endogenous IL-1 inhibitor IL-1Ra instead of the IL-1 cytokines or their receptor our study allowed both to highlight the impact of physiological IL-1 responses by enhancing their potency and to gain valuable insights into their regulation via the IL-1Ra expressed by different subsets of immune cells. Although this approach confirmed the beneficial role of IL-1 in antifungal defense,[16,17] it also exposed the detrimental consequences of macrophage-secreted IL-1Ra for the ability to contain bloodstream *Candida* infection. Moreover, it revealed that the increased inflammation observed

during invasive candidiasis does not reflect excessive signaling via the IL-1R, but the unsuccessful elimination of the fungal pathogen. Collectively, these observations suggest serum IL-1Ra as a future biomarker and potential therapeutic target for invasive candidiasis.

Limitations of the study

We used conditional IL-1Ra-deficient strains that simultaneously deleted all IL-1Ra isoforms by targeting exon 2 of the *IL1rn* gene. We therefore cannot entirely rule out a contribution of intracellular IL-1Ra isoforms to the effects reported in this study. Our analysis of mixed BM chimeras exposed a major role of the secreted IL-1Ra isoform in regulating IL-1-dependent antifungal immunity. Likewise, the fact that we were able to switch the phenotypes of wild-type and IL-1Ra^{Mafb} mice by depleting or reconstituting serum IL-1Ra, respectively, strongly argued for a dominant effect of secreted IL-1Ra. However, targeting approaches that discriminate between the individual IL-1Ra isoforms are needed to further investigate their distinct functions during fungal sepsis.

STAR★METHODS

Detailed methods are provided in the online version of this paper and include the following:

- KEY RESOURCES TABLE
- RESOURCE AVAILABILITY
  - Lead contact
  - Materials availability
  - Data and code availability
- EXPERIMENTAL MODELS
  - Animals
  - *Candida albicans* and inflammation models
- METHOD DETAILS
  - *In vivo* manipulation of splenic macrophages
  - *In vivo* reconstitution and neutralization of IL-1Ra
  - Isolation of leukocyte populations
  - Flow Cytometry analysis
  - Measurement of reactive oxygen species
  - *C. albicans* killing assay
  - Phagocytosis assay
  - Blood sampling
  - Analysis of cytokine responses
  - Western blot analysis
  - Immunohistochemistry and immunofluorescence
  - Quantitative reverse transcription PCR
  - RNA-sequencing and bioinformatics analysis
- QUANTIFICATION AND STATISTICAL ANALYSIS

SUPPLEMENTAL INFORMATION

Supplemental information can be found online at https://doi.org/10.1016/j.immuni.2023.06.023.

ACKNOWLEDGMENTS

We thank Marc Donath and Marianne Böni-Schnetzler (Department of Biomedicine, University Hospital Basel) for kindly providing IL-1Ra^{LysM} mice and recombinant IL-1Ra; Naofumi Mukaida (Kanazawa University, Japan) and Russel Vance (University of California Berkeley, USA) for generously providing the hybridoma-producing IL-1Ra-neutralizing antibody; and Manfred Kopf (ETH Zurich) for kindly sharing the CD11c-Cre strain. We thank the animal caretakers of the Central Animal Facility (Department of Biomedical Research, University of Bern), Stefan Müller and Thomas Schaffer (Flow Cytometry Core Facility, Department of Biomedical Research, University of Bern), Pamela Nicholson (Next Generation Sequencing Platform, University of Bern), Therese Waldburger (Institute of Tissue Medicine and Pathology, University of Bern), and Daniela Sturny (Center for Laboratory Medicine, University Hospital Bern) for excellent technical support. The authors thank Christoph Müller (Institute of Tissue Medicine and Pathology, University of Bern) and Marianne Böni-Schnetzler for reading and commenting on the manuscript. This work was supported by grants from the Swiss National Science Foundation 152872, 197735 (to S.F.), the 3R Research Foundation Switzerland (to S.F.), and the German Research Foundation (DFG) SFB1292, TP13 (to H.C.P.).

AUTHOR CONTRIBUTIONS

H.T.T.G.-B. performed most experiments, analyzed and interpreted the data, prepared the figures, and co-wrote the manuscript. J.S., J.B., and S.W. performed selected experiments and analyzed data. V.G. determined the histopathological grading of tissue sections. G.v.G. and R.B. performed bioinformatics analyses of RNA sequencing data. C.C., J.A.G., and C.G.M. did the immunohistochemistry. M.G., S.M., and H.C.P. conducted experiments in IFNAR-deficient mice. C.G. provided reagents and scientific expertise; S.F. designed and supervised the study, analyzed and interpreted the data, obtained the funding, and wrote the manuscript. All authors read and approved the manuscript.

DECLARATION OF INTERESTS

The authors declare no competing interests.

Received: September 19, 2022
Revised: March 2, 2023
Accepted: June 27, 2023
Published: July 20, 2023

REFERENCES

1. Singer, M., Deutschman, C.S., Seymour, C.W., Shankar-Hari, M., Annane, D., Bauer, M., Bellomo, R., Bernard, G.R., Chiche, J.D., Coopersmith, C.M., et al. (2016). The third international consensus definitions for sepsis and septic shock (Sepsis-3). JAMA *315*, 801–810. https://doi.org/10.1001/jama.2016.0287.
2. Brown, G.D., Denning, D.W., Gow, N.A., Levitz, S.M., Netea, M.G., and White, T.C. (2012). Hidden killers: human fungal infections. Sci. Transl. Med. *4*, 165rv13. https://doi.org/10.1126/scitranslmed.3004404.
3. Wisplinghoff, H., Bischoff, T., Tallent, S.M., Seifert, H., Wenzel, R.P., and Edmond, M.B. (2004). Nosocomial bloodstream infections in US hospitals: analysis of 24,179 cases from a prospective nationwide surveillance study. Clin. Infect. Dis. *39*, 309–317. https://doi.org/10.1086/421946.
4. Kullberg, B.J., and Arendrup, M.C. (2015). Invasive candidiasis. N. Engl. J. Med. *373*, 1445–1456. https://doi.org/10.1056/NEJMra1315399.
5. Pappas, P.G., Lionakis, M.S., Arendrup, M.C., Ostrosky-Zeichner, L., and Kullberg, B.J. (2018). Invasive candidiasis. Nat. Rev. Dis. Primers *4*, 18026. https://doi.org/10.1038/nrdp.2018.26.
6. Lionakis, M.S., and Levitz, S.M. (2018). Host control of fungal infections: lessons from basic studies and human cohorts. Annu. Rev. Immunol. *36*, 157–191. https://doi.org/10.1146/annurev-immunol-042617-053318.
7. Netea, M.G., Joosten, L.A., van der Meer, J.W., Kullberg, B.J., and van de Veerdonk, F.L. (2015). Immune defence against Candida fungal infections. Nat. Rev. Immunol. *15*, 630–642. https://doi.org/10.1038/nri3897.
8. Romani, L. (2011). Immunity to fungal infections. Nat. Rev. Immunol. *11*, 275–288. https://doi.org/10.1038/nri2939.

9. Puel, A. (2020). Human inborn errors of immunity underlying superficial or invasive candidiasis. Hum. Genet. *139*, 1011–1022. https://doi.org/10.1007/s00439-020-02141-7.
10. Desai, J.V., and Lionakis, M.S. (2018). The role of neutrophils in host defense against invasive fungal infections. Curr. Clin. Microbiol. Rep. *5*, 181–189. https://doi.org/10.1007/s40588-018-0098-6.
11. Seagle, E.E., Jackson, B.R., Lockhart, S.R., Georgacopoulos, O., Nunnally, N.S., Roland, J., Barter, D.M., Johnston, H.L., Czaja, C.A., Kayalioglu, H., et al. (2022). The landscape of candidemia during the coronavirus disease 2019 (COVID-19) pandemic. Clin. Infect. Dis. *74*, 802–811. https://doi.org/10.1093/cid/ciab562.
12. Yong, M.K., Slavin, M.A., and Kontoyiannis, D.P. (2018). Invasive fungal disease and cytomegalovirus infection: is there an association? Curr. Opin. Infect. Dis. *31*, 481–489. https://doi.org/10.1097/QCO.0000000000000502.
13. Meizlish, M.L., Franklin, R.A., Zhou, X., and Medzhitov, R. (2021). Tissue homeostasis and inflammation. Annu. Rev. Immunol. *39*, 557–581. https://doi.org/10.1146/annurev-immunol-061020-053734.
14. van der Poll, T., van de Veerdonk, F.L., Scicluna, B.P., and Netea, M.G. (2017). The immunopathology of sepsis and potential therapeutic targets. Nat. Rev. Immunol. *17*, 407–420. https://doi.org/10.1038/nri.2017.36.
15. Dinarello, C.A. (2009). Immunological and inflammatory functions of the interleukin-1 family. Annu. Rev. Immunol. *27*, 519–550. https://doi.org/10.1146/annurev.immunol.021908.132612.
16. Vonk, A.G., Netea, M.G., van Krieken, J.H., Iwakura, Y., van der Meer, J.W., and Kullberg, B.J. (2006). Endogenous interleukin (IL)-1 alpha and IL-1 beta are crucial for host defense against disseminated candidiasis. J. Infect. Dis. *193*, 1419–1426. https://doi.org/10.1086/503363.
17. Bellocchio, S., Montagnoli, C., Bozza, S., Gaziano, R., Rossi, G., Mambula, S.S., Vecchi, A., Mantovani, A., Levitz, S.M., and Romani, L. (2004). The contribution of the Toll-like/IL-1 receptor superfamily to innate and adaptive immunity to fungal pathogens in vivo. J. Immunol. *172*, 3059–3069. https://doi.org/10.4049/jimmunol.172.5.3059.
18. Griffiths, J.S., Camilli, G., Kotowicz, N.K., Ho, J., Richardson, J.P., and Naglik, J.R. (2021). Role for IL-1 family cytokines in fungal infections. Front. Microbiol. *12*, 633047. https://doi.org/10.3389/fmicb.2021.633047.
19. Mantovani, A., Dinarello, C.A., Molgora, M., and Garlanda, C. (2019). Interleukin-1 and related cytokines in the regulation of inflammation and immunity. Immunity *50*, 778–795. https://doi.org/10.1016/j.immuni.2019.03.012.
20. Broderick, L., and Hoffman, H.M. (2022). IL-1 and autoinflammatory disease: biology, pathogenesis and therapeutic targeting. Nat. Rev. Rheumatol. *18*, 448–463. https://doi.org/10.1038/s41584-022-00797-1.
21. Arend, W.P., Malyak, M., Guthridge, C.J., and Gabay, C. (1998). Interleukin-1 receptor antagonist: role in biology. Annu. Rev. Immunol. *16*, 27–55. https://doi.org/10.1146/annurev.immunol.16.1.27.
22. Palomo, J., Dietrich, D., Martin, P., Palmer, G., and Gabay, C. (2015). The interleukin (IL)-1 cytokine family–Balance between agonists and antagonists in inflammatory diseases. Cytokine *76*, 25–37. https://doi.org/10.1016/j.cyto.2015.06.017.
23. Aksentijevich, I., Masters, S.L., Ferguson, P.J., Dancey, P., Frenkel, J., van Royen-Kerkhoff, A., Laxer, R., Tedgård, U., Cowen, E.W., Pham, T.H., et al. (2009). An autoinflammatory disease with deficiency of the interleukin-1-receptor antagonist. N. Engl. J. Med. *360*, 2426–2437. https://doi.org/10.1056/NEJMoa0807865.
24. Broz, P., and Dixit, V.M. (2016). Inflammasomes: mechanism of assembly, regulation and signalling. Nat. Rev. Immunol. *16*, 407–420. https://doi.org/10.1038/nri.2016.58.
25. Latz, E., Xiao, T.S., and Stutz, A. (2013). Activation and regulation of the inflammasomes. Nat. Rev. Immunol. *13*, 397–411. https://doi.org/10.1038/nri3452.
26. Chan, A.H., and Schroder, K. (2020). Inflammasome signaling and regulation of interleukin-1 family cytokines. J. Exp. Med. *217*, e20190314. https://doi.org/10.1084/jem.20190314.
27. He, Y., Hara, H., and Núñez, G. (2016). Mechanism and regulation of NLRP3 inflammasome activation. Trends Biochem. Sci. *41*, 1012–1021. https://doi.org/10.1016/j.tibs.2016.09.002.
28. Lamacchia, C., Palmer, G., Bischoff, L., Rodriguez, E., Talabot-Ayer, D., and Gabay, C. (2010). Distinct roles of hepatocyte- and myeloid cell-derived IL-1 receptor antagonist during endotoxemia and sterile inflammation in mice. J. Immunol. *185*, 2516–2524. https://doi.org/10.4049/jimmunol.1000872.
29. Böni-Schnetzler, M., Häuselmann, S.P., Dalmas, E., Meier, D.T., Thienel, C., Traub, S., Schulze, F., Steiger, L., Dror, E., Martin, P., et al. (2018). β Cell-Specific Deletion of the IL-1 Receptor Antagonist Impairs β Cell Proliferation and insulin Secretion. Cell Rep. *22*, 1774–1786. https://doi.org/10.1016/j.celrep.2018.01.063.
30. Martin, P., Palmer, G., Rodriguez, E., Palomo, J., Lemeille, S., Goldstein, J., and Gabay, C. (2020). Intracellular IL-1 receptor antagonist Isoform 1 released from keratinocytes upon cell death acts as an inhibitor for the alarmin IL-1α. J. Immunol. *204*, 967–979. https://doi.org/10.4049/jimmunol.1901074.
31. Lamacchia, C., Palmer, G., Seemayer, C.A., Talabot-Ayer, D., and Gabay, C. (2010). Enhanced Th1 and Th17 responses and arthritis severity in mice with a deficiency of myeloid cell-specific interleukin-1 receptor antagonist. Arthritis Rheum. *62*, 452–462. https://doi.org/10.1002/art.27235.
32. Clausen, B.E., Burkhardt, C., Reith, W., Renkawitz, R., and Förster, I. (1999). Conditional gene targeting in macrophages and granulocytes using LysMcre mice. Transgenic Res. *8*, 265–277. https://doi.org/10.1023/a:1008942828960.
33. Wu, X., Briseño, C.G., Durai, V., Albring, J.C., Haldar, M., Bagadia, P., Kim, K.W., Randolph, G.J., Murphy, T.L., and Murphy, K.M. (2016). Mafb lineage tracing to distinguish macrophages from other immune lineages reveals dual identity of Langerhans cells. J. Exp. Med. *213*, 2553–2565. https://doi.org/10.1084/jem.20160600.
34. Caton, M.L., Smith-Raska, M.R., and Reizis, B. (2007). Notch-RBP-J signaling controls the homeostasis of CD8- dendritic cells in the spleen. J. Exp. Med. *204*, 1653–1664. https://doi.org/10.1084/jem.20062648.
35. van Rooijen, N., Kors, N., and Kraal, G. (1989). Macrophage subset repopulation in the spleen: differential kinetics after liposome-mediated elimination. J. Leukoc. Biol. *45*, 97–104. https://doi.org/10.1002/jlb.45.2.97.
36. Fujioka, N., Mukaida, N., Harada, A., Akiyama, M., Kasahara, T., Kuno, K., Ooi, A., Mai, M., and Matsushima, K. (1995). Preparation of specific antibodies against murine IL-1RA and the establishment of IL-1RA as an endogenous regulator of bacteria-induced fulminant hepatitis in mice. J. Leukoc. Biol. *58*, 90–98. https://doi.org/10.1002/jlb.58.1.90.
37. Müller, U., Steinhoff, U., Reis, L.F., Hemmi, S., Pavlovic, J., Zinkernagel, R.M., and Aguet, M. (1994). Functional role of type I and type II interferons in antiviral defense. Science *264*, 1918–1921. https://doi.org/10.1126/science.8009221.
38. Ioannou, M., Hoving, D., Aramburu, I.V., Temkin, M.I., De Vasconcelos, N.M., Tsourouktsoglou, T.D., Wang, Q., Boeing, S., Goldstone, R., Vernardis, S., et al. (2022). Microbe capture by splenic macrophages triggers sepsis via T cell-death-dependent neutrophil lifespan shortening. Nat. Commun. *13*, 4658. https://doi.org/10.1038/s41467-022-32320-1.
39. Brown, G.D. (2011). Innate antifungal immunity: the key role of phagocytes. Annu. Rev. Immunol. *29*, 1–21. https://doi.org/10.1146/annurev-immunol-030409-101229.
40. Warnatsch, A., Tsourouktsoglou, T.D., Branzk, N., Wang, Q., Reincke, S., Herbst, S., Gutierrez, M., and Papayannopoulos, V. (2017). Reactive oxygen species localization programs inflammation to clear microbes of different size. Immunity *46*, 421–432. https://doi.org/10.1016/j.immuni.2017.02.013.
41. Van't Wout, J.W., Van der Meer, J.W., Barza, M., and Dinarello, C.A. (1988). Protection of neutropenic mice from lethal Candida albicans infection by recombinant interleukin 1. Eur. J. Immunol. *18*, 1143–1146. https://doi.org/10.1002/eji.1830180728.
42. Kullberg, B.J., van 't Wout, J.W., and van Furth, R. (1990). Role of granulocytes in increased host resistance to Candida albicans induced by

recombinant interleukin-1. Infect. Immun. *58*, 3319–3324. https://doi.org/10.1128/iai.58.10.3319-3324.1990.

43. Smeekens, S.P., Ng, A., Kumar, V., Johnson, M.D., Plantinga, T.S., van Diemen, C., Arts, P., Verwiel, E.T., Gresnigt, M.S., Fransen, K., et al. (2013). Functional genomics identifies type I interferon pathway as central for host defense against Candida albicans. Nat. Commun. *4*, 1342. https://doi.org/10.1038/ncomms2343.

44. Majer, O., Bourgeois, C., Zwolanek, F., Lassnig, C., Kerjaschki, D., Mack, M., Müller, M., and Kuchler, K. (2012). Type I interferons promote fatal immunopathology by regulating inflammatory monocytes and neutrophils during Candida infections. PLoS Pathog. *8*, e1002811. https://doi.org/10.1371/journal.ppat.1002811.

45. del Fresno, C., Soulat, D., Roth, S., Blazek, K., Udalova, I., Sancho, D., Ruland, J., and Ardavín, C. (2013). Interferon-β production via Dectin-1-Syk-IRF5 signaling in dendritic cells is crucial for immunity to C. albicans. Immunity *38*, 1176–1186. https://doi.org/10.1016/j.immuni.2013.05.010.

46. Biondo, C., Signorino, G., Costa, A., Midiri, A., Gerace, E., Galbo, R., Bellantoni, A., Malara, A., Beninati, C., Teti, G., et al. (2011). Recognition of yeast nucleic acids triggers a host-protective type I interferon response. Eur. J. Immunol. *41*, 1969–1979. https://doi.org/10.1002/eji.201141490.

47. Domínguez-Andrés, J., Feo-Lucas, L., Minguito de la Escalera, M., González, L., López-Bravo, M., and Ardavín, C. (2017). Inflammatory Ly6C high monocytes protect against candidiasis through IL-15-driven NK cell/neutrophil activation. Immunity *46*, 1059–1072.e4. https://doi.org/10.1016/j.immuni.2017.05.009.

48. Guarda, G., Braun, M., Staehli, F., Tardivel, A., Mattmann, C., Förster, I., Farlik, M., Decker, T., Du Pasquier, R.A., Romero, P., et al. (2011). Type I interferon inhibits interleukin-1 production and inflammasome activation. Immunity *34*, 213–223. https://doi.org/10.1016/j.immuni.2011.02.006.

49. Stawowczyk, M., Naseem, S., Montoya, V., Baker, D.P., Konopka, J., and Reich, N.C. (2018). Pathogenic effects of IFIT2 and interferon-β during fatal systemic Candida albicans infection. mBio *9*, e00365-18. https://doi.org/10.1128/mBio.00365-18.

50. Ji, D.X., Yamashiro, L.H., Chen, K.J., Mukaida, N., Kramnik, I., Darwin, K.H., and Vance, R.E. (2019). Type I interferon-driven susceptibility to Mycobacterium tuberculosis is mediated by IL-1RA. Nat. Microbiol. *4*, 2128–2135. https://doi.org/10.1038/s41564-019-0578-3.

51. Mayer-Barber, K.D., Andrade, B.B., Oland, S.D., Amaral, E.P., Barber, D.L., Gonzales, J., Derrick, S.C., Shi, R., Kumar, N.P., Wei, W., et al. (2014). Host-directed therapy of tuberculosis based on interleukin-1 and type I interferon crosstalk. Nature *511*, 99–103. https://doi.org/10.1038/nature13489.

52. Castiglia, V., Piersigilli, A., Ebner, F., Janos, M., Goldmann, O., Damböck, U., Kröger, A., Weiss, S., Knapp, S., Jamieson, A.M., et al. (2016). Type I interferon signaling prevents IL-1β-driven lethal systemic hyperinflammation during invasive bacterial infection of soft tissue. Cell Host Microbe *19*, 375–387. https://doi.org/10.1016/j.chom.2016.02.003.

53. Mayer-Barber, K.D., and Yan, B. (2017). Clash of the Cytokine Titans: counter-regulation of interleukin-1 and type I interferon-mediated inflammatory responses. Cell. Mol. Immunol. *14*, 22–35. https://doi.org/10.1038/cmi.2016.25.

54. McNab, F., Mayer-Barber, K., Sher, A., Wack, A., and O'Garra, A. (2015). Type I interferons in infectious disease. Nat. Rev. Immunol. *15*, 87–103. https://doi.org/10.1038/nri3787.

55. Gross, O., Gewies, A., Finger, K., Schäfer, M., Sparwasser, T., Peschel, C., Förster, I., and Ruland, J. (2006). Card9 controls a non-TLR signalling pathway for innate anti-fungal immunity. Nature *442*, 651–656. https://doi.org/10.1038/nature04926.

56. Gross, O., Poeck, H., Bscheider, M., Dostert, C., Hannesschläger, N., Endres, S., Hartmann, G., Tardivel, A., Schweighoffer, E., Tybulewicz, V., et al. (2009). Syk kinase signalling couples to the Nlrp3 inflammasome for anti-fungal host defence. Nature *459*, 433–436. https://doi.org/10.1038/nature07965.

57. Gringhuis, S.I., Kaptein, T.M., Wevers, B.A., Theelen, B., van der Vlist, M., Boekhout, T., and Geijtenbeek, T.B. (2012). Dectin-1 is an extracellular pathogen sensor for the induction and processing of IL-1β via a noncanonical caspase-8 inflammasome. Nat. Immunol. *13*, 246–254. https://doi.org/10.1038/ni.2222.

58. Saijo, S., Ikeda, S., Yamabe, K., Kakuta, S., Ishigame, H., Akitsu, A., Fujikado, N., Kusaka, T., Kubo, S., Chung, S.H., et al. (2010). Dectin-2 recognition of alpha-mannans and induction of Th17 cell differentiation is essential for host defense against Candida albicans. Immunity *32*, 681–691. https://doi.org/10.1016/j.immuni.2010.05.001.

59. Pfeifer, J., Thurner, B., Kessel, C., Fadle, N., Kheiroddin, P., Regitz, E., Hoffmann, M.C., Kos, I.A., Preuss, K.D., Fischer, Y., et al. (2022). Autoantibodies against interleukin-1 receptor antagonist in multisystem inflammatory syndrome in children: a multicentre, retrospective, cohort study. Lancet Rheumatol. *4*. e329–e337. https://doi.org/10.1016/S2665-9913(22)00064-9.

60. Jarrell, J.A., Baker, M.C., Perugino, C.A., Liu, H., Bloom, M.S., Maehara, T., Wong, H.H., Lanz, T.V., Adamska, J.Z., Kongpachith, S., et al. (2022). Neutralizing anti-IL-1 receptor antagonist autoantibodies induce inflammatory and fibrotic mediators in IgG4-related disease. J. Allergy Clin. Immunol. *149*, 358–368. https://doi.org/10.1016/j.jaci.2021.05.002.

61. Kyriazopoulou, E., Huet, T., Cavalli, G., Gori, A., Kyprianou, M., Pickkers, P., Eugen-Olsen, J., Clerici, M., Veas, F., Chatellier, G., et al. (2021). Effect of anakinra on mortality in patients with COVID-19: a systematic review and patient-level meta-analysis. Lancet Rheumatol. *3*. e690–e697. https://doi.org/10.1016/S2665-9913(21)00216-2.

62. Tahtinen, S., Tong, A.J., Himmels, P., Oh, J., Paler-Martinez, A., Kim, L., Wichner, S., Oei, Y., McCarron, M.J., Freund, E.C., et al. (2022). IL-1 and IL-1RA are key regulators of the inflammatory response to RNA vaccines. Nat. Immunol. *23*, 532–542. https://doi.org/10.1038/s41590-022-01160-y.

63. Shakoory, B., Carcillo, J.A., Chatham, W.W., Amdur, R.L., Zhao, H., Dinarello, C.A., Cron, R.Q., and Opal, S.M. (2016). Interleukin-1 receptor blockade is associated with reduced mortality in sepsis patients with features of macrophage activation syndrome: reanalysis of a prior phase III trial. Crit. Care Med. *44*, 275–281. https://doi.org/10.1097/CCM.0000000000001402.

64. Caffrey, A.K., Lehmann, M.M., Zickovich, J.M., Espinosa, V., Shepardson, K.M., Watschke, C.P., Hilmer, K.M., Thammahong, A., Barker, B.M., Rivera, A., et al. (2015). IL-1α signaling is critical for leukocyte recruitment after pulmonary Aspergillus fumigatus challenge. PLoS Pathog. *11*, e1004625. https://doi.org/10.1371/journal.ppat.1004625.

65. Godwin, M.S., Reeder, K.M., Garth, J.M., Blackburn, J.P., Jones, M., Yu, Z., Matalon, S., Hastie, A.T., Meyers, D.A., and Steele, C. (2019). IL-1RA regulates immunopathogenesis during fungal-associated allergic airway inflammation. JCI Insight *4*, e129055. https://doi.org/10.1172/jci.insight.129055.

66. Candon, S., Rammaert, B., Foray, A.P., Moreira, B., Gallego Hernanz, M.P., Chatenoud, L., and Lortholary, O. (2020). Chronic disseminated candidiasis during hematological malignancies: an immune reconstitution inflammatory syndrome with expansion of pathogen-specific T helper type 1 cells. J. Infect. Dis. *221*, 1907–1916. https://doi.org/10.1093/infdis/jiz688.

67. Dellière, S., Guery, R., Candon, S., Rammaert, B., Aguilar, C., Lanternier, F., Chatenoud, L., and Lortholary, O. (2018). Understanding pathogenesis and care challenges of immune reconstitution inflammatory syndrome in fungal infections. J. Fungi (Basel) *4*, 139. https://doi.org/10.3390/jof4040139.

68. Srinivas, S., Watanabe, T., Lin, C.S., William, C.M., Tanabe, Y., Jessell, T.M., and Costantini, F. (2001). Cre reporter strains produced by targeted insertion of EYFP and ECFP into the ROSA26 locus. BMC Dev. Biol. *1*, 4. https://doi.org/10.1186/1471-213x-1-4.

69. Swamydas, M., Luo, Y., Dorf, M.E., and Lionakis, M.S. (2015). Isolation of mouse neutrophils. Curr. Protoc. Immunol. *110*, 3.20.1–3.20.15. https://doi.org/10.1002/0471142735.im0320s110.

Please cite this article in press as: Gander-Bui et al., Targeted removal of macrophage-secreted interleukin-1 receptor antagonist protects against lethal *Candida albicans* sepsis, Immunity (2023), https://doi.org/10.1016/j.immuni.2023.06.023

STAR★METHODS

KEY RESOURCES TABLE

REAGENT or RESOURCE	SOURCE	IDENTIFIER
Antibodies		
Biotin anti-mouse CD19	Biolegend	Cat#115504; RRID:AB_313639
Biotin anti-mouse CD3ε	Biolegend	Cat#100304; RRID:AB_312669
Biotin anti-mouse CD49b	Biolegend	Cat#108904; RRID:AB_313411
Biotin anti-mouse Ly-6G	Biolegend	Cat#127604; RRID:AB_1186108
Biotin anti-mouse NK-1.1	Biolegend	Cat#108704; RRID:AB_313391
Biotin anti-mouse CD317	Biolegend	Cat#127006; RRID:AB_2028466
Biotin anti-mouse CD11c	Biolegend	Cat#117304; RRID:AB_313773
Biotin anti-mouse Ly-6C	Biolegend	Cat#128003; RRID:AB_1236552
Biotin anti-mouse CD90.2	Biolegend	Cat#105304; RRID:AB_313175
Biotin anti-mouse F4/80	Biolegend	Cat#123106; RRID:AB_893501
Biotin anti-mouse Siglec-F	Miltenyi	Cat#130-118-959; RRID:AB_2733493
Biotin anti-TER-119/Erythroid Cells	Biolegend	Cat#116204; RRID:AB_313705
Biotin anti-mouse CD25 Antibody	Biolegend	Cat#102004; RRID:AB_312853
Biotin anti-mouse I-A/I-E Antibody	Biolegend	Cat#107603; RRID:AB_313318
Biotin anti-mouse/human CD45R/B220	Biolegend	Cat#103204; RRID:AB_312989
Purified anti-mouse CD16/32	Biolegend	Cat#101302; RRID:AB_312801
Brilliant Violet 605™ anti-mouse Ly-6G	Biolegend	Cat#127639; RRID:AB_2565880
FITC anti-mouse Ly-6G	Biolegend	Cat#127606; RRID:AB_1236494
PE anti-mouse F4/80	Biolegend	Cat#123110; RRID:AB_893486
Brilliant Violet 510™ anti-mouse I-A/I-E	Biolegend	Cat#107636; RRID:AB_2734168
FITC anti-mouse CD45.1	Biolegend	Cat#110706; RRID:AB_313495
Brilliant Violet 711™ anti-mouse CD45.1	Biolegend	Cat#110739; RRID:AB_2562605
Brilliant Violet 711™ anti-mouse CD45.2	Biolegend	Cat#109847; RRID:AB_2616859
APC/Cy7 anti-mouse CD11c	Biolegend	Cat#117323; RRID:AB_830646
PE/Cy7 anti-mouse CD11c	Biolegend	Cat#117318; RRID:AB_493568
PE anti-mouse CD115	Biolegend	Cat#135506; RRID:AB_1937253
PerCP/Cyanine5.5 anti-mouse/ human CD11b	Biolegend	Cat#101228; RRID:AB_893232
PE/Cy7 anti-mouse/human CD11b	Biolegend	Cat#101216; RRID:AB_312799
Brilliant Violet 711™ Streptavidin	Biolegend	Cat#405241
Brilliant Violet 421™ Streptavidin	Biolegend	Cat#405226
Super Bright 436 anti-mouse Siglec-F	eBioscience™	Cat#62-1702-80; RRID:AB_2664258
FITC anti-mouse CD45R/B220	Biolegend	Cat#103206; RRID:AB_312991
PE anti-mouse CD101	eBioscience™	Cat#12-1011-82; RRID:AB_1210728
Alexa Fluor 647 anti-mouse CD169	Biolegend	Cat#142408; RRID:AB_2563621
PE goat anti-rat Ig	SouthernBiotech	Cat#3010-09; RRID:AB_2795804
anti-mouse MARCO	Bio-Rad Laboratories	Cat#MCA 1849; RRID:AB_322923
Anti-mouse Phospho-p38 MAPK (Thr180/ Tyr182)	Cell Signaling	Cat#9211S; RRID:AB_331641
Anti-mouse p38 MAPK	Bio-Rad Laboratories	Cat#9212S; RRID:AB_330713
Anti-mouse β-Actin	SantaCruz	Cat#sc-47778; RRID:AB_626632
Anti-IL-1β Monoclonal Antibody (B122)	eBioscience™	Cat#14-7012-85; RRID:AB_468397
IL-1β Polyclonal Antibody, Biotin	eBioscience™	Cat#13-7112-85; RRID:AB_466925
Streptavidin-AP	SouthernBiotech	Cat#7105-04

(*Continued on next page*)

Please cite this article in press as: Gander-Bui et al., Targeted removal of macrophage-secreted interleukin-1 receptor antagonist protects against lethal *Candida albicans* sepsis, Immunity (2023), https://doi.org/10.1016/j.immuni.2023.06.023

Continued

REAGENT or RESOURCE	SOURCE	IDENTIFIER
Anti-mouse IL-1 beta /IL-1F2	RnD	Cat#AB-401-NA; RRID:AB_354347
Anti-mouse IL-1 alpha /IL-1F1	RnD	Cat#AB-400-NA; RRID:AB_354346
Anti-mouse IL-1Ra	RnD	Cat#AF-480-NA; RRID:AB_2125574
Anti-mouse IL-1Ra	Invitrogen	Cat#PA5-21776; RRID:AB_11154011
Anti-mouse IL-1Ra monoclonal antibody	This paper	Hybridoma provided by Naofumi Mukaida
Anti-mouse IL-1RI	RnD	Cat#BAF771; RRID:AB_356713
Anti-mouse MPO	Agilent-Dako	Cat#A0398; RRID:AB_2335676
Anti-mouse F4/80	Bio-Rad Laboratories	Cat#MCA 497; RRID:AB_2098196
Anti-mouse CD68	Abcam	Cat#ab125212; RRID:AB_10975465
Anti-mouse GFP	Novus	Cat#NB600-308; RRID:AB_10003058
m-IgG Fc BP-HRP	SantaCruz	Cat#sc-525409
Goat anti-rabbit IgG-HRP	SantaCruz	Cat#sc-2030; RRID:AB_631747
Bovine anti-goat IgG-HRP	SantaCruz	Cat#sc-2352; RRID:AB_634812
Rabbit Anti-Rat IgG H&L	Abcam	Cat#ab102248
Fixable Viability Dye eFluor™ 780	Invitrogen	Cat#65-0865-14
Anti-CD11b MicroBeads	Miltenyi Biotec	Cat#130-049-601; RRID:AB_2927377
Anti-CD11c MicroBeads	Miltenyi Biotec	Cat#130-108-338
Ultra-LEAF Purified Armenian Hamster IgG Isotype Antibody	Biolegend	Cat#400940; RRID:AB_11203529
DAPI	Sigma-Aldrich	Cat#D9542
Purified anti-mouse IL-6 (ELISA capture, clone MP5-20FS)	eBioscience	Cat#14-7061-85; RRID:AB_468423
IL-6 monoclonal antibody (MP5-32C11), biotin	eBioscience	Cat#13-7062-85; RRID:AB_466911
PE/Cyanine7 anti-mouse CD63 Antibody	Biolegend	Cat#143910; RRID:AB_2565500
IL-1 beta (Pro-form) Monoclonal Antibody (NJTEN3), APC	eBioscience	Cat#17-7114-80; RRID:AB_10670739
Alexa Fluor® 647 anti-mouse Ly-6C Antibody	Biolegend	Cat#128010; RRID:AB_1236550
MPO, Mouse, mAb 8F4, FITC	Hycult Biotech	Cat#HM1051F; RRID:AB_2146341
Anti-Histone H3 (citrulline R2 + R8 + R17) antibody	Abcam	Cat#Ab5103; RRID:AB_304752
Recombinant Mouse IFN-β1 (carrier-free)	Biolegend	Cat#581304
Rabbit anti-Goat IgG (H+L) Cross-Adsorbed Secondary Antibody, Alexa Fluor™ 546	Invitrogen	Cat#A21085; RRID:AB_2535742
Recombinant Anti-CCR2 antibody [EPR20844-15]	Abcam	Cat#ab273050; RRID:AB_2893307
Recombinant Anti-Iba1 antibody [EPR16588]	Abcam	Cat#ab178846; RRID:AB_2636859
Recombinant Anti-Ly6G antibody [EPR22909-135]	Abcam	Cat#ab238132; RRID:AB_2923218
Streptavidin-AP	Southern Biotech	Cat#7100-04
Bacterial and virus strains		
C. albicans SC5314 strain		N/A
Lymphocytic choriomeningitis virus (LCMV) WE strain		N/A
Vesicular stomatitis virus (VSV Indiana)		N/A
Listeria monocytogenes 10403S strain		N/A
Vaccinia virus		N/A

(*Continued on next page*)

Please cite this article in press as: Gander-Bui et al., Targeted removal of macrophage-secreted interleukin-1 receptor antagonist protects against lethal *Candida albicans* sepsis, Immunity (2023), https://doi.org/10.1016/j.immuni.2023.06.023

Continued

REAGENT or RESOURCE	SOURCE	IDENTIFIER
Chemicals, peptides, and recombinant proteins		
Zymosan A from *Saccharomyces cerevisiae*	Sigma Aldrich	Cat# Z4250
pHrodo™ Green Zymosan A BioParticles™	Invitrogen	Cat# P35365
Lipopolysaccharides from Escherichia coli	InvivoGen	Cat# tlrl-eblps
Lipopolysaccharide from *E.coli* O111: B4	Sigma Aldrich	Cat# L3012
Polyinosinic-polycytidylic acid (PIC)	InvivoGen	Cat# tlrl-pic
YPD broth	BD	Cat# 242820
YPD agar	BD	Cat# 242720
BHI broth	BD	Cat# 237500
RPMI-1640 Medium	Sigma Aldrich	Cat# R0883
HEPES solution	Sigma Aldrich	Cat# H0887
MEM Non-essential Amino Acid Solution	Sigma Aldrich	Cat# M7145
L-Glutamine solution	Sigma Aldrich	Cat# G7513
Fetal Bovine Serum	Sigma Aldrich	Cat# F7524
Percoll®	Sigma Aldrich	Cat# GE17-0891-01
Lympholyte®-M	Cederlane	Cat# CL5035
Liberase TM	Sigma Aldrich	Cat# 5401127001
DNAse I from bovine pancreas	Sigma Aldrich	Cat# DN25-1G
Collagenase IV	Worthington	Cat# LS004189
cOmplete™ ULTRA Tablets	Roche	Cat# 5892970001
Phosphatase Inhibitor Cocktail 2	Sigma Aldrich	Cat# P5726
Phosphatase Inhibitor Cocktail 3	Sigma Aldrich	Cat# P0044
PMSF Protease Inhibitor	Sigma Aldrich	Cat# 93842
Recombinant mouse IL-1RA protein	Abcam	Cat# ab119723
Recombinant Mouse IL-1RA (IL-1RN)	Biolegend	Cat# 769704
Recombinant human IL-1Ra (anakinra)	a gift from Marianne Böni-Schnetzler	N/A
Recombinant Murine IL-1β	PeProtech	Cat# 211-11B
Recombinant Mouse IL-1β/IL-1F2 Protein	RnD	Cat# 401-ML-010
Recombinant Mouse IFN-β Protein	RnD	Cat# 8234-MB-010
TRIzol™ Reagent	ThermoFisher	Cat# 15596026
KAPA SYBR® FAST	Sigma Aldrich	Cat# KK4601
Murine RNase Inhibitor, 15'000 units	New England BioLabs	Cat# M0314L
Ambion™ DNase I (RNase-free)	ThermoFisher	Cat# AM2222
GoScript™ Reverse Transcriptase	Promega Helix	Cat# A5003
Clodronate Liposomes	Liposoma Inc	Cat# C-005
2′,7′-Dichlorofluorescein	Sigma Aldrich	Cat# D6665
Liquemin Inj Loos 25000 U / 5ml	Drossapharm	N/A
Ethylenediaminetetraacetic acid disodium salt solution (EDTA) 0.5M	Sigma Aldrich	Cat# E7889
D-galactosamine HCl	Carbosynth	Cat# MGO050301701
para-Nitrophenylphosphate (pNPP)	Sigma Aldrich	Cat# N2765-100TAB
Bovine Serum Albumin	Sigma Aldrich	Cat# A4503
NOPIL child syrup.Sulfamethoxazole /Trimethoprim 200 / 40mg	Mepha Pharma AG	N/A
TRI Reagent®	Zymo Research	Cat# R2050-1-50
Direct-zol™ RNA miniprep Plus kit	Zymo Research	Cat# R2070
ReliaPrep RNA cell miniprep System	Promega	Cat# Z6011
EasySep™ Mouse Neutrophil Enrichment Kit	StemCell Technologies	Cat# 19762
EasySep Mouse Monocyte Isolation Kit	StemCell Technologies	Cat# 19861
Dako Fluorescence mounting medium	Dako	Cat# S3023

(*Continued on next page*)

Please cite this article in press as: Gander-Bui et al., Targeted removal of macrophage-secreted interleukin-1 receptor antagonist protects against lethal *Candida albicans* sepsis, Immunity (2023), https://doi.org/10.1016/j.immuni.2023.06.023

Continued

REAGENT or RESOURCE	SOURCE	IDENTIFIER
Mouse IL-6, recombinant protein	eBioscience	Cat# 14-8061-80
dNTP-Mix	Seraglob by Bioswisstec AG	Cat# 1910-002
Random Nonamers	Sigma Aldrich	Cat# R7647
1-Brom-3-chlorpropan	Sigma Aldrich	Cat# B9673
2-Propanol	Sigma Aldrich	Cat# 278475
Triton™ X-100	Sigma Aldrich	Cat# T8787
Tween 20	Sigma Aldrich	Cat# P1379
Dihydrorhodamin 123	Sigma Aldrich	Cat# D1054
SuperSignal™ West Pico chemiluminescent substrate	ThermoFisher	Cat# 34577
BBL Thioglycollate medium brewer modified	BD	Cat# 211716
Critical commercial assays		
Mouse IL-1ra/IL-1F3 DuoSet ELISA	RnD	Cat# DY480
Mouse G-CSF DuoSet ELISA	RnD	Cat# DY414-05
PrimeFlow™ RNA assay	ThermoFisher	Cat# 88-18005-204
IL1RN PrimeFlow probe set-Alexa Fluor 647	ThermoFisher	Cat# PF-210 (VB1-3028457-PF)
Mouse Cytokine/Chemokine 31-Plex Discovery Assay® Array	Eve Technologies	N/A
Qubit RNA BR Assay Kit	ThermoFisher	Cat# Q10210
Fragment Analyzer Systems RNA Kit	Agilent	Cat# DNF-471-0500
CORALL Total RNA-Seq V2 library Prep.kit	Lexogen	N/A
RiboCop rRNA Depletion Kit	Lexogen	N/A
JetSeq™ Library Quantification Lo-ROX Kit	Bioline	Cat# BIO-68029
NovaSeq 6000 S1 Reagent Kit v1.5 (300 cycles)	Illumine	Cat# 20028317
Pierce® BCA Protein Assay Kit	ThermoFisher	Cat# 23225
Deposited data		
Bulk RNA sequencing data	This paper	ENA: E-MTAB-12997
Experimental models: Organisms/strains		
Mouse: C57BL/6J	The Jackson Laboratory	JAX000664
Mouse: CD45.1 (B6.SJL-PtprcaPepcb/BoyJ)	The Jackson Laboratory	JAX002014
Mouse: Mafb-Cre (Mafbtm1.1(cre)Kmm/J)	The Jackson Laboratory	JAX029664
Mouse: R26R-EYFP (B6.129X1-Gt(ROSA) 26Sortm1(EYFP)Cos/J)	The Jackson Laboratory	JAX006148
Mouse: IL-1Rafl/fl (Il1rntm1.1Cga)	Lamacchia et al.[31]	N/A
Mouse: LysM-Cre (Lyz2tm1(cre)Ifo/J)	Clausen et al.[32]	N/A
Mouse: CD11c-Cre (B6.Cg-Tg(Itgax-cre) 1-1Reiz)	Caton et al.[34]	N/A
Mouse: B6.129S2-Ifnar1tm1Agt/Mmjax	The Jackson Laboratory	JAX101830
Oligonucleotides		
See Table S1 for qPCR primers	This paper	N/A
Software and algorithms		
FlowJo software (version 10.8.1)		N/A
GraphPad PRISM (version 9.1.0)		N/A
R version 4.1.0		N/A
Aperio ImageScope (v12.4.0.5043)		N/A

Please cite this article in press as: Gander-Bui et al., Targeted removal of macrophage-secreted interleukin-1 receptor antagonist protects against lethal *Candida albicans* sepsis, Immunity (2023), https://doi.org/10.1016/j.immuni.2023.06.023

RESOURCE AVAILABILITY

Lead contact

Further information and requests for resources and reagents should be directed to the lead contact, Stefan Freigang (stefan.freigang@unibe.ch).

Materials availability

This study did not generate new unique reagents.

Data and code availability

RNA-seq data have been deposited at ENA and are publicly available as of the date of publication. Accession numbers are listed in the key resources table. Microscopy data reported in this paper will be shared by the lead contact upon request.

This paper does not report original code.

Any additional information required to reanalyze the data reported in this paper is available from the lead contact upon request.

EXPERIMENTAL MODELS

Animals

Mice were bred and maintained in specific-pathogen-free (SPF) facilities at the Institute of Tissue Medicine and Pathology of the University of Bern. All procedures were performed in accordance with ethical guidelines and approved animal license protocols of the Canton of Bern (BE3/18 and BE31/2021). Mice were housed with a 12 h light/dark cycle, regulated temperature and humidity, and provided unlimited access to food and water. C57BL/6J, CD45.1 (B6.SJL-PtprcaPepcb/BoyJ), Mafb-Cre (Mafbtm1.1(cre)Kmm/J),[33] and R26R-EYFP (B6.129X1-Gt(ROSA)26Sortm1(EYFP)Cos/J)[68] mice were purchased from The Jackson Laboratory and bred in-house. IL-1Ra^{LysM} mice had been generated[31] by crossing IL-1Ra$^{fl/fl}$ (Il1rntm1.1Cga) mice[31] to LysM-Cre (Lyz2tm1(cre)Ifo/J) mice[32] and were kindly provided by Marc Donath (Department of Biomedicine, University Hospital Basel). To obtain IL-1Ra^{Mafb} and IL-1Ra^{CD11c} mice, we crossed IL-1Ra$^{fl/fl}$ mice with Mafb-Cre or CD11c-Cre (B6.Cg-Tg(Itgax-cre)1-1Reiz)[34] mice, respectively. CD11c-Cre mice were a gift from Manfred Kopf (Institute of Molecular Health Sciences, ETH Zurich). In general, IL-1Ra$^{fl/fl}$ Cre-negative littermates served as controls; for some experiments IL-1Ra$^{wt/wt}$ Cre-positive mice were used as controls and yielded wild type results. R26R-EYFP mice (termed EYFP^{LSL} here) were crossed with LysM-Cre, Mafb-Cre, or CD11c-Cre mice to create the respective EYFP-Cre-reporter strains, which we referred to as EYFP^{LysM}, EYFP^{Mafb}, or EYFP^{CD11c} here. All mouse strains were backcrossed onto C57BL/6 for more than 10 generations or had been generated on a C57BL/6 background. Age- and sex-matched animals were randomly assigned to experimental groups. To generate bone marrow (BM) chimeras (BMC), six-week-old recipient mice were lethally γ-irradiated using a GammaCell X40 irradiator 24 hours prior to intravenous injection of 5x10^6 donor BM cells. Mice received sulfamethoxazole and trimethoprim via the drinking water for two weeks, and were rested for at least eight weeks to allow BM reconstitution before performing the experiments.

Candida albicans and inflammation models

C. albicans (SC5413) was grown in YPD medium (BD Difco™ YPD Broth, BD Sciences) at 30°C for 18 hours. *C. albicans* yeast cells were washed twice in sterile PBS and counted using a hemocytometer. To obtain *C. albicans* hyphae, washed *C. albicans* yeast were cultured in RPMI 1640 (10% FBS) at 37°C for 4 h. Heat-killed yeast and hyphae were prepared by incubation at 72°C for 1 h, and complete inactivation was confirmed by plating on YPD agar plates at 30°C for 48 h. For *in vivo* experiments, eight- to ten-week-old mice were infected intravenously with 0.5 - 2.5x10^5 colony forming units (CFU) *C. albicans* via the lateral tail vein. To determine fungal organ titers, mice were euthanized, and organs were weighed and homogenized in 0.5% NP-40 water with a TissueLyser II (Qiagen) at 25 Hz for 2x 3 min. Serial dilutions of tissue homogenates in PBS were then plated onto YPD agar, incubated for 24 - 48 h, and fungal burden was calculated as CFU *C. albicans*/g tissue. To assess the effect of type I IFN on IL-1Ra production and *C. albicans* infection *in vivo*, mice were injected with 2 μg of mouse recombinant IFN-β (Biolegend) alone, and with the synthetic TLR3 ligand polyinosinic-polycytidylic acid (PIC, InvivoGen) either alone or 5 hours prior to *C. albicans* infection. Similarly, mice were infected with 1x10^4 or 2x10^6 plaque forming units (pfu) lymphocytic choriomeningitis virus (LCMV) strain WE, either alone or one day before infection with *C. albicans*. Production of IL-1Ra in spleen and serum was also assessed at day 1 p.i. with 10^6 pfu vesicular stomatitis virus (VSV Indiana), 2x10^6 pfu vaccinia virus (VV) or 3000 CFU Listeria monocytogenes (strain 10403S). Pathogens were diluted from frozen viral stocks grown in MDCK cells (VV), BHK21 cells (LCMV WE), Vero cells (VSV), or prepared freshly as overnight cultures in brain heart infusion broth (Listeria). To evaluate early cell recruitment induced by fungal components, mice were intraperitoneally injected with 1 mg of Zymosan A from Saccharomyces cerevisiae (Sigma) freshly dissolved in sterile PBS. At 6 h and 18 h post injection, blood and peritoneal exudates were collected. Serum and peritoneal lavage fluid were stored at -80°C prior to IL-1Ra measurement by ELISA. Leukocytes in blood and peritoneal lavage were characterized by flow cytometry. Peritoneal neutrophils were purified from lavage using magnetic bead-based isolation before assessing *C. albicans* killing and phagocytosis *in vitro*. To assess LPS-induced IL-1Ra expression, mice were intraperitoneally injected with ultra-pure LPS O111:B4 (150 μg/kg, Sigma) and D-galalactosamine (800 mg/kg, Carbosynth Ltd.), and serum and organs were collected 5 h later.

Please cite this article in press as: Gander-Bui et al., Targeted removal of macrophage-secreted interleukin-1 receptor antagonist protects against lethal *Candida albicans* sepsis, Immunity (2023), https://doi.org/10.1016/j.immuni.2023.06.023

METHOD DETAILS

In vivo manipulation of splenic macrophages

Splenectomy was performed under isoflurane anesthesia in a laminar flow bench. The abdominal skin and peritoneal membrane were opened by two small incisions to expose the spleen. The spleen was removed by cauterizing the splenic arteries and veins at the splenic hilum. The peritoneal membrane was closed with absorbable suture and skin incision was closed with wound clips. After the surgery, mice were allowed to recover under a heating lamp and rested for eight weeks before *C. albicans* infection. To selectively deplete macrophages of the splenic marginal zone, mice were intravenously injected with commercial clodronate liposomes (Liposoma) at 1 mg per animal, while control mice received an equal volume of sterile PBS. Ten days later, all mice were infected with 2.5 x10^5 CFU *C. albicans*. Serum and organs were harvested at day 3 p.i. for analysis.

In vivo reconstitution and neutralization of IL-1Ra

Recombinant human IL-1Ra (anakinra) was a gift from Marianne Böni-Schnetzler (Department of Biomedicine, University Hospital Basel). IL-1Ra^{Mafb} mice received recombinant IL-1Ra (500 μg per mouse) intraperitoneally twice daily on days 0, 1, and 2 post *C. albicans* infection. Non-reconstituted IL-1Ra$^{fl/fl}$ and IL-1Ra^{Mafb} mice in these experiments received injections of an equal volume of sterile PBS. The hybridoma producing a neutralizing anti-mouse IL-1Ra antibody[36] was generously provided by Naofumi Mukaida (Kanazawa University, Japan) and Russell Vance (University of California Berkeley, USA). Monoclonal antibody was produced and purified in-house using protein G resin (GenScript). For preventive IL-1Ra neutralization *in vivo*, mice received intraperitoneal injections of either neutralizing anti-IL-1Ra antibody or control Ultra-LEAF purified armenian hamster IgG isotype antibody (BioLegend) on days -1, 1 and 2 of infection. For therapeutic IL-1Ra neutralization, mice were administered intravenously anti-IL-1Ra or control antibody on days 2 to 6 post *C. albicans* infection.

Isolation of leukocyte populations

Leukocytes were isolated from kidneys by a modification of the protocol of Swamydas et al.[69] Kidneys were dissected into 1 mm^3 pieces using a scalpel, digested in 6 ml of serum-free RPMI 1640 medium with 0.2 mg/ml of Liberase™ (Roche) and 0.2 mg/ml DNase I (Sigma) for 45 min at 37°C. At the end of the incubation, an equal volume of complete RPMI 1640 medium was added; the cell suspension was filtered through a 40 μm cell strainer, and washed twice in PBS. The pellet was then suspended in 40% Percoll (Sigma), gently overlaid onto 70% Percoll and centrifuged at 880 g at room temperature for 30 min. Splenic single cell suspensions were obtained by enzymatic digestion with 2 mg/ml of type IV collagenase (Worthington) and 0.2 mg/ml DNAse I (Sigma) for 45 min at 37°C. Neutrophils were purified using the EasySep™ Mouse Neutrophil Enrichment Kit (StemCell Technologies) supplemented with biotinylated antibodies (all BioLegend) as following: anti-CD3ε (3.45 μg/ml), anti-B220 (2.5 μg/ml), anti-TER119 (0.25 μg/ml), anti-F4/80 (3.45 μg/ml), anti-CD11c (3.45 μg/ml), anti-CD19 (3.45 μg/ml), anti-NK1.1 (3.45 μg/ml) and anti-CD317 (2.5 μg/ml). Monocytes were isolated using the EasySep™ Mouse Monocyte Isolation Kit (StemCell Technologies) using biotinylated antibodies (all BioLegend) at the following final concentrations: anti-CD3ε (3.45 μg/ml), anti-B220 (2.5 μg/ml), anti-TER119 (0.25 μg/ml), anti-F4/80 (3.45 μg/ml), anti-CD19 (3.45 μg/ml), anti-NK1.1 (3.45μg/ml) and anti-CD317 (2.5 μg/ml). For the analysis of the gene expression or *in vitro* IL-1Ra production of individual leukocyte subsets, single cell suspensions were first prepared from infected organs as described above. Following cell surface staining to identify leukocyte subsets, cells of individual mice were FACS-purified on a MoFlo Astrios EQ sorter (Beckman Coulter) by the flow cytometry core facility at the Department of Biomedical Research, University of Bern. Cells were sorted into pre-warmed complete medium. BM cells were collected by flushing femur and tibia from both hind legs with sterile PBS. Erythrocytes were lysed using ACK lysis buffer, before primary BM neutrophils and BM monocytes were isolated using the EasySep™ Mouse Neutrophil Enrichment Kit and EasySep™ Mouse Monocyte Isolation Kit as stated above. For *in vitro* analysis of LPS-induced IL-1Ra production, splenic macrophages and splenic dendritic cells were purified from single cell suspensions using magnetic anti-CD11b MicroBeads and CD11c MicroBeads (Miltenyi Biotec) according to the manufacturer's instructions. BM-derived macrophages we generated by culturing BM cells in complete RPMI 1640 medium supplemented with 10% L929 cell supernatant as a source of M-CSF. Medium was exchanged every 3 days, and BM-derived macrophages were harvested for experiments on day 7. Peritoneal macrophages were harvested 4 days after intraperitoneal instillation of 1 ml 3.8% thioglycollate (Becton Dickinson AG). Lavage cells were washed with PBS and cultured overnight in the presence or absence of 10 ng/ml LPS (InvivoGen). IL-1Ra production was then assessed in culture supernatants by ELISA or in cell lysates by western blot.

Flow Cytometry analysis

Single cell suspensions were prepared as described above and stained with live/dead dye (Invitrogen) and anti-mouse CD16/32 antibody (BioLegend) for 15 min at 4°C. Immune cell subsets were characterized using antibodies against CD90, CD19, CD49b, CD45, CD11b, CD11c, F4/80, Ly-6C, Ly-6G, I-A/I-E, and CD115 (all BioLegend), as well as against CD101 (eBioscience™) and Siglec F (Miltenyi Biotec) as published[47] (Figure S4D). Neutrophils, resident macrophages, Ly-6^{hi} monocytes, Ly-6C^{lo} monocytes and DCs were defined as CD45$^+$ CD11b$^+$ Ly-6G^{hi}, CD45$^+$ CD11b$^+$ F4/80$^+$, CD45$^+$ CD11b$^+$ F4/80$^-$ MHCII$^-$ Ly6C^{hi}, CD45$^+$ CD11b$^+$ F4/80$^-$ MHCII$^-$ Ly6C$^-$ CD11c$^+$, and CD45$^+$ CD11b$^+$ F4/80$^-$ MHC$^+$ CD11c$^+$, respectively. Blood mature neutrophils, immature neutrophils and monocytes were identified as CD11b$^+$ CD115- Ly6G$^+$ CD101$^+$, CD11b$^+$ CD115$^-$ Ly6G$^+$ CD101$^-$ and CD11b$^+$ CD115$^+$ Ly6C$^+$, respectively. For phenotypic characterization of neutrophils, cells were stained with antibodies against CD45.2, CD11b, Ly-6G, CD63 (all BioLegend), CD101 and pro-IL-1beta (both from eBioscience™) and MPO (Hycult Biotech). Cell populations were positive for

CD90, CD19, CD49b, CD11c, F4/80, I-A/I-E and Siglec-F, were excluded from the flow cytometry analysis. Cells were fixed in 4% paraformaldehyde (PFA) for 5 min before acquisition. Intracellular IL-1Ra transcripts in kidney-infiltrating leukocytes were revealed using the PrimeFlow™ RNA assay (Thermo Fisher) according to the manufacturer's instructions. After cell surface staining for CD45.2, CD11b, CD11c, MHC II, F4/80, Ly-6C and Ly-6G, cells were fixed and permeabilized, followed by the hybridization with the *Il1rn* probe, signal amplification and fluorescence labeling. All samples were acquired on a LSRII cytometer (BD Biosciences) and analyzed using FlowJo (BD Biosciences).

Measurement of reactive oxygen species

Freshly purified neutrophils (10^6 per well) were equilibrated for 60 min at 37°C before staining with 5 μM 2',7'-dichlorofluorescein (DCF) in serum-free RPMI for 30 min, followed by exposure to heat-killed *C. albicans* (MOI 3) in the presence or absence of IL-1β (20 ng/ml) for additional 30 min. Cells were then stained with live/dead fluorescent dye and antibodies against CD45.2, CD11b, Ly-6G, and Ly6C. ROS production was quantified in leukocytes isolated from the blood, spleen and kidneys of *C. albicans* infected mice. Cells were incubated for 30 min at 37°C with Dihydrorhodamine 123 (Sigma Aldrich) before staining with live/dead fluorescent dye and antibodies against CD45.2, CD11b, Ly-6G, Ly-6C, and CD101. Frequencies of ROS producing neutrophils were analyzed using FlowJo (BD Biosciences).

C. albicans killing assay

To test fungicidal capacity, 5 x10^4 neutrophils were incubated with 2 x 10^4 *C. albicans* for 3 h. Cells were then lysed with 1% NP-40 water and serial dilutions of the lysates were plated on YPD agar. Colonies were counted after 24 h at 30°C. Fungicidal capacity was expressed as the percentage of *C. albicans* inoculum detected in control wells without leukocytes, that was killed in presence of neutrophils.

Phagocytosis assay

Phagocytosis activity was measured using pHrodo™ Green Zymosan Bioparticles (Thermo Fisher) according to the manufacturer's instructions. Neutrophils were purified from peritoneal cavities of Zymosan A-primed mice, plated in black clear bottom 96-well plates (Corning) at 10^5 cells/well in 100 μl Opti-MEM® (Gibco), and equilibrated at 37°C for 1 h. Culture medium was then replaced by 100 μl of 0.5 mg/ml pHrodo™ Green Zymosan Bioparticles in uptake buffer and incubation continued for 2 h at 37°C in the presence or absence of IL-1β (20 ng/ml). Bioparticles in pH 5.0 buffer served as positive control. Bioparticle-free wells and wells containing Bioparticles in uptake buffer served as background and negative control. Fluorescence intensity was assessed with excitation at 490 nm and emission at 535 nm using an Infinite M200 pro Tecan microplate reader. Net phagocytosis was calculated by correcting for fluorescence intensity of background and negative controls. Phagocytosis is expressed as percentage of net fluorescence intensity in experimental wells as compared to the net positive control.

Blood sampling

Blood samples were collected terminally from the vena cava into syringes containing heparin (for creatinine and blood urea nitrogen) or EDTA (for cytokine analyses) as anticoagulant. All samples were kept on ice while handling. Blood was transferred to blood collection tubes (BD microtainer) for serum isolation or 1.5 ml reaction tubes for plasma collection and centrifuged for 10 min at 2000 g at 4°C. 100 μl of resulting supernatants were transferred into clean polypropylene tubes and processed directly or stored at -80°C until analysis. Measurement of plasma creatinine and blood urea nitrogen concentrations was performed by the Center for Laboratory Medicine at the University Hospital Bern.

Analysis of cytokine responses

Cytokine concentrations in serum, peritoneal lavages or cell culture supernatants were determined by ELISA. Production of IL-1Ra and G-CSF in serum and culture supernatant were measured using the mouse IL-1ra/IL-1F3 DuoSet kit and the mouse G-CSF DuoSet kit (RnD Systems), according to the manufacturer's guidelines. Mouse IL-1β and IL-6 were quantified using sandwich ELISA with an anti-IL-1β / biotinylated anti-IL-1β or anti-IL-6 / biotinylated anti-IL-6 antibody pairs (all from eBioscience), respectively, followed by detection with streptavidin-alkaline phosphatase (Southern Biotech) and para-nitrophenylphosphate. Optical densities were read on an Infinite M200 pro Tecan microplate reader and concentrations were calculated using recombinant standards for mouse IL-1β (RnD Systems) and IL-6 (eBioscience), respectively. Cytokine profiles in infected kidneys were characterized with a Mouse Cytokine/Chemokine 31-Plex Discovery Assay® Array (Eve Technologies). In brief, infected kidneys were snap-frozen, homogenized in modified RIPA buffer, and tissue homogenates were stored at -80°C until analysis.

Western blot analysis

Purified leukocyte subsets were lysed in modified RIPA buffer (50 mM Tris HCl pH 7.4, 150 mM NaCl, 1% NP-40, 0.5% Triton X100, 1 mM EDTA, 0.5% sodium deoxycholate, 0.1% SDS, and 10 mM NaF), supplemented with protease inhibitors (Roche), phenylmethylsulfonylfluoride, and phosphatase inhibitor cocktail 2 and 3 (Sigma Aldrich). Protein extracts were normalized using the Pierce® BCA Protein Assay Kit (Thermo Fisher); and 25 μg of protein were assessed by reducing SDS-PAGE (10-12%). After transfer onto polyvinylidene difluoride (PVDF) membranes (Bio-Rad Laboratories), immunoblotting was performed with anti-IL-1Ra (Thermo Fisher), anti-p38, anti-phospho-p38 (both Cell Signaling), and anti-β actin (Santa Cruz Biotechnology) primary antibodies and

Please cite this article in press as: Gander-Bui et al., Targeted removal of macrophage-secreted interleukin-1 receptor antagonist protects against lethal *Candida albicans* sepsis, Immunity (2023), https://doi.org/10.1016/j.immuni.2023.06.023

corresponding HRP-conjugated secondary antibodies (Santa Cruz), followed by development in SuperSignal™ West Pico chemiluminescent substrate. Staining was visualized using a ChemiDoc™ MP Imaging System (Bio-Rad Laboratories).

Immunohistochemistry and immunofluorescence

Organs were dissected and fixed in 4% paraformaldehyde for 6 to 8 h, followed by standard paraffin embedding. Tissue sections (2.5 μm) were stained on an Immunostainer Leica Bond RX (Leica Biosystems) with periodic acid-Schiff (PAS), with methenamine silver (Grocott), or with anti-IL-1Ra, anti-IL-1α, anti-IL-1β, anti-IL-1R1 (all R&D Systems), anti-F4/80 (Bio-Rad Laboratories), anti-CD68, anti-Ly-6G, anti-CCR2, anti-Iba1, anti-Histone H3 (citrulline R2+R8+R17) (all from Abcam), anti-MPO (Agilent) or anti-GFP (Novus) antibodies. Embedding, sectioning and staining were performed by the Translational Research Unit of the Institute of Pathology at the University of Bern. Images were obtained with a Pannoramic 250 scanner (3DHistech) before analysis. Histological grading was performed on Periodic acid-Schiff (PAS) stained sections by a trained pathologist blinded to the identity of the specimens. Inflammation and *C. albicans* dissemination were evaluated separately for the tubulointerstitial compartment and glomeruli. Scores ranging from 0 to 3 were defined for each category and criterion, as described below. The final score of each section represents the sum of the scores for the tubulointerstitial compartment and the glomeruli.

	Inflammation		*Candida* dissemination	
Score	Tubulointerstitial compartment	Glomeruli	Tubulointerstitial compartment	Glomeruli
0	No inflammation	No inflammation	No *Candida*	No *Candida*
1	Focal tubulointerstitial inflammation	Minimal	Few *Candida*	Few *Candida*
2	Single abscess	Moderate	Abundant *Candida*	Abundant *Candida*
3	Multiple abscesses	Severe	Massive *Candida*	Massive *Candida*

Spleen tissue was frozen in OCT medium and cut (5 μm) on a Leica CM1950 cryostat. Acetone-fixed cryosections were incubated in PBS containing 10% goat serum and 0.1% Triton X-100 (Sigma-Aldrich) to block nonspecific binding for 1h, before staining with anti-mouse MARCO (Bio-Rad Laboratories) and anti-mouse CD169 (BioLegend) antibodies overnight. Rinsed sections were stained with DAPI (Sigma Aldrich) for 20 minutes, and then mounted with Dako Fluorescence Mounting Medium (Dako). Fluorescent images were acquired using a Pannoramic 250 flash II slide scanner (3DHistech). IL-1Ra-positive areas in stained kidney sections were quantified using ImageScope (v12.4.0.5043). To visualize the colocalization of marginal zone macrophages and IL-1Ra, spleen tissue was frozen in OCT medium and cut (10 μm) on a Leica CM1950 cryostat. PFA-fixed (4%) cryosections treated with multistaining buffer (Lunaphore) were stained using the LabSat technology (Lunaphore). In the first cycle anti-mouse CD169 (Biolegend), anti-mouse IL1RA (R & D Systems) with secondary rabbit anti-goat Alexa Fluor 546 antibody (Invitrogen) and DAPI were stained and imaged. After applying the quenching buffer (Lunaphore), in the second cycle, MARCO (Bio-Rad Laboratories) with corresponding secondary antibody (PE goat anti-rat Ig, SouthernBiotech) and DAPI was stained and imaged.

Quantitative reverse transcription PCR

Kidneys were disrupted in 0.5 to 1 ml of TRIzol Reagent (Ambion Life Technologies) with stainless steel beads (5 mm; Qiagen) in a TissueLyser II (Qiagen) for 2 cycles of 2 min at 25Hz. Total mRNA was isolated according to manufacturer's instructions. Contaminating DNA was digested by RNase-free DNase (Life Technologies), mRNA concentrations were measured with a NanoDrop™ One spectrophotometer (Thermo Fisher) and 1 μg mRNA/reaction was reverse-transcribed using GoScript™ Reverse Transcriptase (Promega) in presence of RNase inhibitor (BioLabs). Quantitative PCR was performed using KAPA SYBR® FAST qPCR Master Mix (2X) Kit (Sigma) on a StepOnePlus™ Real-Time PCR System (Thermo Fisher), and expression was normalized to *G6pdx* or *Actb* expression. For FACS-sorted cells, RNA was purified using the ReliaPrep™ RNA Miniprep Systems (Promega) following the manufacturers' instructions.

RNA-sequencing and bioinformatics analysis

Kidneys of infected mice were harvested at day 2 p.i., snap-frozen in liquid nitrogen before homogenization in TRI Reagent® (Zymo Research) in BashingBeat™ lysis tubes (Zymo Research) with a TissueLyser II (Qiagen) for 3 cycles of 1 min at 30Hz. Total RNA was extracted using the Direct-zol™ RNA miniprep Plus kit (Zymo Research) and stored at -80°C until use. The quantity and quality of the purified total RNA was assessed using a Qubit 4.0 fluorometer with the Qubit RNA BR Assay Kit (Thermo Fisher) and an Advanced Analytical Fragment Analyzer System using a Fragment Analyzer RNA Kit (Agilent), respectively. Two hundred ng of input RNA was first depleted of ribosomal RNA and globin mRNA using RiboCop for HMR+ Globin Depletion Kit (Lexogen) following the manufacturer's instructions. Thereafter, cDNA libraries were generated using a CORALL Total RNA-Seq V2 library Prep.kit with UDIs 12nt set A1 (Lexogen) according to the protocol for long insert sizes. The quantity and length of the cDNA libraries were investigated using the Qubit 4.0 fluorometer and Advanced Analytical Fragment Analyzer System as above. Library quantification was also determined using a JetSeq library Quantification Lo-ROX kit (Bioline) following the manufacturer's instructions. Equimolar-pooled cDNA libraries

were sequenced paired-end using an illumina NovaSeq 6000 S1 Reagent Kit v1.5 (300 cycles) on an illumina NovaSeq 6000 instrument (illumina). The run produced between 50-60 million reads/sample. The quality of the sequencing run was assessed using illumina Sequencing Analysis Viewer (illumina, version 2.4.7) and all base call files were demultiplexed and converted into FASTQ files using illumina bcl2fastq conversion software v2.20. The quality control assessments, generation of libraries and sequencing was carried out at the Next Generation Sequencing Platform, University of Bern. From the raw sequencing reads, adapters and poly(A) sequences were removed with cutadapt (v3.4). After that, 12 bp UMI sequences were extracted and high error rate sequences were removed with UMI-tools (v1.2.2) according to the suggestions of the manufacturer of the library preparation kit. Reads were aligned with hisat2 (v2.2.1) to the ensemble mouse genome (GRCm38.p6). Read alignments were deduplicated with UMI-tools (v1.2.2). The counting of fragments aligning to genic features was performed with featureCounts (v2.0.1) based on the ensembl mouse gene annotation v102. DESeq2 was used to calculate differential gene expression out of the raw count matrices. Gene set enrichment analysis (GSEA) was performed with the R package clusterProfiler based on gene ordering according to the test statistic acquired from the differential gene expression results of DESeq. Gene Ontology overrepresentation analysis was performed with the R package topGO on genes which were differentially expressed with an adjusted p-value smaller than 0.05. Heatmap visualizations were generated with the R package ComplexHeatmap. All downstream analyses in R were performed with R version 4.1.0.

QUANTIFICATION AND STATISTICAL ANALYSIS

Unless data of individual mice are shown, data represent mean ± SEM. Statistical analyses were performed using the GraphPad Prism software. Two-tailed Student's t-test, one-way ANOVA with a Bartlett's multiple comparisons test or two-way ANOVA with a Tukey's multiple comparisons test were applied to compare two or several groups as specified in figure legends. Statistical significance was considered as $p < 0.05$. Asterisks denote statistical significance (*, $p < 0.05$; **, $p < 0.01$; ***, $p < 0.001$; ****, $p < 0.0001$).